Ratcheting behavior of sensitized non-conventional austenitic stainless steel

Thesis submitted in partial fulfillment of the requirements for the degree

of

Master of Technology
in
Mechanical Engineering
[Steel Technology]

Submitted By

Antara Bhattacharjee

Roll No- 213MM2481

Department of Metallurgical and Materials Engineering
National Institute of Technology
Rourkela-769008
2015

Ratcheting behavior of sensitized non-conventional austenitic stainless steel

Thesis submitted in partial fulfillment of the requirements for the degree
of

Master of Technology
in
Mechanical Engineering
[Steel Technology]

Submitted By

Antara Bhattacharjee

Roll No- 213MM2481

Under Supervision of
Prof. Krishna Dutta

Department of Metallurgical and Materials Engineering
National Institute of Technology
Rourkela-769008

2015

National Institute of Technology, Rourkela

Certificate

This is to certify that the thesis entitled, **"*Ratcheting behavior of sensitized non-conventional austenitic stainless steel"*** submitted by ***Antara Bhattacharjee*** in partial fulfillment of the requirements for the award of the degree of **Master of Technology** in **Mechanical Engineering** with Specialization of **Steel Technology** at the **National Institute of Technology, Rourkela** is an authentic work carried out by her under my supervision and guidance.

To the best of my knowledge, the matter embodied in the thesis has not been submitted to any other University/ Institute for the award of any degree or diploma.

Date:

Place: Rourkela

Supervisor

Prof. Krishna Dutta

Department of Metallurgical and Materials Engineering

National institute of Technology, Rourkela-769008

Acknowledgements

I express my deep sense of gratitude, profound respect and indebtedness to my guide **Professor Krishna Dutta**, Department of Metallurgical and Materials Engineering, National Institute of Technology Rourkela, for providing precious guidance, inspiring discussions and constant supervision throughout the course of this work being carried out. His timely help, constructive criticism and conscientious efforts made it possible to present the work contained in this report.

I am sincerely thankful to **Professor S. C. Mishra,** Head of the department Metallurgical and Materials Engineering, NIT Rourkela, **Professor B. B. Verma** and other faculty members of the department for their persistent support and advice during the course work. I am also cordially grateful to **Professor K. K. Ray**, Department of Metallurgical and Materials Engineering, IIT Kharagpur, for his priceless help during the course of this research work. I also express my sincere gratitude to **Professor Debashish Sarkar** of Ceramic Engineering and **Professor Snehanshu Pal**, Department of Metallurgical and Materials Engineering who have helped me in every possible way through their kind consent and valuable suggestions.

I am also thankful to the technical assistants – **Mr. S. Hembram**, **Mr. A. Acharya** and **Mr. K. Tanty**, Department of Metallurgical and Materials Engineering, for their assistance and all sorts of help while conducting the experiments.

I am thankful to **Mr. Lala Amarnath** for his sincere help throughout the project.

Date:

Place: Rourkela **Antara Bhattacharjee**

Contents

Abstract

The aim of this investigation is to study the effect of ratcheting behaviour on a sensitized non-conventional austenitic stainless steel. The metallurgical investigation of solution annealed as well as sensitized stainless steels were carried out in order to determine the microstructural characteristics, hardness, grain size distribution, tensile properties, ratcheting behaviour and post-ratcheting tensile properties of differently heat treated stainless steel specimens. The microstructural examinations have been done with the help of optical microscope and scanning electron microscope (SEM). The microstructure of the selected steel in solution annealed condition reveals that the steel owns nearly equiaxed austenite grains with annealing twins throughout the matrix. The phenomenon of plastic strain accumulation due to asymmetric cyclic loading is known as ratcheting. Stress-controlled cyclic loading experiments have been carried out at room temperature for constant mean stress levels with varying stress amplitudes after each 50 cycles. Cyclic loading rate for stress control test is 50 MPa/s. The stress, nominal strain and the actuator displacement data were continuously recorded during each test to obtain at least 200 data points per cycle. Ratcheting deformation is found to increase with increase in stress amplitude values for constant values of stress mean. However, the rate of strain accumulation increases with increasing stress amplitude. The analyses of stress-strain results indicate that the steel cyclically softens in both solution annealed as well as sensitized conditions. This nature of softening is also seen in the post-fatigue tensile tested samples. The yield strength and tensile strength value of unratcheted tensile as well as post ratcheted tensile steel samples were found to reduce. The fractographic analyses indicate that the fracture surfaces of the sensitized specimens are predominantly of typical rock candy type fracture whereas dimple fracture was observed in the solution annealed sample. The X-Ray diffraction (XRD) analyses using Cu Kα radiation attributes to in-situ martensitic transformation during deformation. It was noticed that the phase transformation plays a significant role on the variation in tensile strength of the steel.

Key Words: Non-conventional stainless steel, sensitization, solution annealed, ratcheting, stress amplitude, in-situ martensitic transformation

List of Figures

List of Tables

CHAPTER 1

Introduction

1.1 Introduction

Stainless steel, from over a century, has become a vitally significant material; its fantabulous compounding of mechanical, corrosion and oxidation resistance properties make it perfect for use in a varied range of different environs and circumstances [1]. Austenitic stainless steel is a grade of stainless steel having 16-25% chromium and sufficient amount of austenite-stabilizing elements like manganese, nickel, or nitrogen, so that the steel is austenitic even at room temperature [2]. These are used in a wide range of applications owing to its non-magnetic nature, excellent toughness even at low temperatures as there is no ductile to brittle transition and good ductility with elongation of not less than or about 50% in tensile tests [3]. These steels find its use in nuclear, petro-chemical, chemical industries and many more.

A very common phenomenon called thermal sensitization is usually found associated with these steels when they are held at the temperature range of 550°C-750°C during the service or welding. This leads to the precipitation of carbides and/or nitrides at the grain boundaries, particularly chromium carbide (generally $Cr_{23}C_6$) in the alloy while chromium depletion occurs from the neighboring zones. This makes them susceptible to intergranular stress corrosion cracking (IGSCC) or intergranular corrosion (IGC) [4]. Therefore, microstructural changes are brought about in these stainless steels while successively affecting its resistance to corrosion as well as their mechanical properties. Earlier researches on sensitization of various materials have divulged the nature of precipitation, the precipitation kinetics and the aging behavior involved [5]. The increase in deterioration of ductility and fracture toughness of the AISI 304LN grade stainless steel with an increase in the degree of sensitization has already been established while studies reveal that degree of sensitization have almost no effect on the values of the tensile strength of the steel specimens [6]. Some studies also indicate that sensitization of austenitic stainless steel contributes to the formation of martensite as a result of the deformation induced in them.

The AISI 304 grade of austenitic stainless steel is largely used in heat transfer pipelines of heavy water reactors at nuclear power plants as well as in chemical industries. These pipelines may be exposed to high temperatures for prolonged time or may be cyclically loaded due to temblor or sometimes both. Therefore, it is understood that austenitic stainless steels are widely used in various industrial sectors. In all these sectors it is very prone to fatigue kind of deformation as well as get sensitized. The current investigation is done using a non conventional (ISO/TR 15510 X12CrMnNiN17-7-5) austenitic stainless steel, similar in properties to AISI 304 grade of steels, especially developed to preserve nickel, and thus making it economical. This non-conventional stainless steel however can be used in various automotive parts like trim, wheel covers, flat conveyor chains, rail-road passenger car bodies etc., and various structural as well as architectural applications. Moreover, it is expected that sensitization also has effect on the mechanical properties of the stainless steel. As per the knowledge of the current investigator, no research has been done to understand the effect of sensitization on the mechanical properties of this austenitic stainless steel. Further on this non-conventional steel no work has been done to reveal the consequences of sensitization treatment on the mechanical properties especially tensile and fatigue properties.

In recent days, a new stream of low cycle fatigue has become the interest of the research community. This new type of fatigue behavior is known as ratcheting which occurs under the influence of asymmetric cyclic loading. Occurrences of continuous accruement of inelastic strain when a material is subjected to cyclical loading characterized by non-zero mean stress is called ratcheting. Cycle-by-cycle ratcheting strain increases progressively and it may cause ruinous effect [7]. Therefore it is very crucial to know the ratcheting behavior of the engineering components or structures to safe guard them during their service life. However, most existing reports on ratcheting behavior of stainless steel are lined with experimental fatigue life and life prediction models as well as some variations in the material's substructural features [8]. However no published report exists on the ratcheting behavior of sensitized stainless steel. This report aims to fulfill the gap [7,8].

1.2 Objectives of the research work

The major objectives and relevant work plans to fulfill these can be briefly summed as:

a) To impart thermal sensitization treatment on the selected steel samples.

b) To characterize the differentially heat treated steel samples.

c) To study the ratcheting and post ratcheting behavior of the steel samples.

d) To investigate the in-situ transformation of austenite due to deformation.

CHAPTER 2

Literature Review

2.1 Stainless Steel-An Over View

Riley of Glasgow, in 1889 discovered that on additions of nickel, tensile strength of mild steel increased significantly. In 1905 *Portevin* noticed that steels with chromium content more that 9 weight% were resistant to acid attack. *Brearly of Sheffield* sought to preclude fouling and corrosion in rifle barrels by utilizing ferritic iron-chrome alloys which were resistant to metallographic etchants. He named these alloys "*stainless steels*" and subsequently they became the foundation of the cutlery trade since 1914 [3].

In America and Europe, the advances in manufacture and fabrication technology resulted in large-scale applications of austenitic and ferritic steels for ammonia and nitric acid plants from 1925. In due course of time the amount of production of austenitic steels exceeded any of the ferritic alloys, thus concentrating more research and development effort on the former. Austenitic steels are now broadly used in various modern engineering plant such as steam power plant, gas turbine, fusion and fission reactor plant, jet propulsion units and chemical plant. Stainless steels have a minimum of 11.5 weight% chromium which forms a thin stable and protective oxide film on the surface due to its strong affinity for oxygen. The imperviousness and passiveness of this oxide layer restricts further reaction with the encompassing atmosphere [3]. The steel attains pleasant appearance, corrosion resistance and resistance to oxidation due to the presence of chromium. There are other alloying elements apart from chromium such as nickel, manganese and molybdenum which improves various properties including corrosion resistance. Stainless steels can be used in diverse applications due to the combination of the following properties:

- Good creep resistance at elevated temperature due to their low stacking fault energy which prevents easy cross-slip of screw dislocations.
- Resistant to corrosion and oxidation even in an oxidizing atmosphere.
- Resistant to scaling and oxidation at raised temperature.

- High formability and ductility.
- Superior machinability and weldability.
- Good toughness at low temperatures as no ductile to brittle transition occurs in austenitic stainless steel [2].

Stainless steel could be divided into five categories and they are:

- *Ferritic stainless steel* – chromium is the major alloying element with 11.5-27 weight% and have ferritic structure upto melting point. The other alloying elements are manganese, silicon, nickel, aluminium, molybdenum and titanium. The carbon content is kept as low as possible to enhance toughness and reduce the chances of sensitization. Their complete freedom from stress-corrosion makes them more useful in chemical plants. Due to their lack of toughness in weld, these steels are limited in use to comparatively thin sections.
- *Martensitic stainless steel* – heat-treatable steels containing 12-17% chromium and 0.10-1.20% carbon. These are similar to ferritic steels except for the higher carbon content. These are austenite at a temperature range of 950-1000°C but are transformed to martensite on cooling. To enhance the yield strength value upto 550-1680 MPa these are tempered and hardened. These are put into use where high strength and moderate corrosion resistance is required. They are magnetic but have normally low formability and weldability.
- *Austenitic stainless steel* – stainless steels having 16-25% chromium and enough of austenite stabilizing elements (nickel, manganese and/or nitrogen) which make the structure austenitic even at room temperature. Nickel is the austenite stabilizer in AISI 300 series alloys whereas when manganese partly/fully replaces nickel it is the AISI 200 series alloys. Austenitic stainless steels have a tendency to stress corrosion cracking in presence of even very less amount of chloride ions. The failures can occur in presence of small applied stresses in mild corrosive atmosphere. The fracture is of transgranular nature with negligible amount of plastic deformation. Due to the fcc structure at room temperature, these alloys are non-magnetic in nature, tough even at low temperatures and good ductility. These are used in nuclear, petro-chemical and

chemical industries due to their non-magnetic character, fantabulous ductility, toughness even at sub-zero temperature. They are widely used as piping components in chemical and nuclear industries where they have to sustain high temperature exposure for a continuous time period. During their service life, austenitic stainless steels are often met with the problem of sensitization.

- *Duplex stainless steel* – their microstructure contains approximately 50% ferritic and 50% austenitic. This provides them a superior strength as compared to both ferritic and austenitic steels. These are resistant to stress corrosion cracking and hence known as "lean duplex" steels as they are formulated to have equivalent corrosion resistance as compared to standard austenitic steels but improved strength and resistance to stress corrosion cracking. "Super duplex" steels have increased strength and resistance to corrosion as compared to austenitic steels. They are weldable and have moderate formability. They are magnetic but not as high as the ferritic and martensitic steels due to the presence of 50% austenitic phase.
- *Precipitation-hardenable stainless steels* – presence of alloying elements such as copper, niobium and aluminium increases strength. Very fine particle matrix is produced in the steel by providing suitable ageing treatment which further enhances strength. They can be machined to produce intricate shapes requiring good tolerances [1].

Stainless steels are used in varied applications owing to their versatile nature. These are:

- **Domestic** – cutlery, saucepans, sinks, microwave oven liners, washing machine drums, razor blades.
- **Transport** – exhaust systems, car trim/grilles, road tankers, ship containers, ships chemical tankers, refuse vehicles.
- **Architectural/Civil Engineering** –handrails, cladding, street furniture, door and window fittings, structural sections, lighting columns, reinforcement bar, masonry supports, lintels.
- **Medical** – Surgical instruments, surgical implants, MRI scanners.

- **Chemical/Pharmaceutical** – pressure vessels, process piping.
- **Oil and Gas** – platform accommodation, cable trays, subsea pipelines.
- **Food and Drink** – Catering equipment, brewing, distilling, food processing.
- **Water** – Water and sewage treatment, water tubing, hot water tanks.
- **General** – springs, fasteners, wire [1].

2.2 Sensitization of Stainless Steel

It is been known from past half a century that stainless steel are vulnerable to a form of corrosion known as inter granular corrosion. In his early works, Bain et al. stated that "one of the little shortcomings of the austenitic stainless steels is that the metal, after exposure to reasonably high temperatures in the range of 1000-1500°F, has been regularly found to be subjected to a very typical form of intergranular corrosion, even in environments which generally have no effect upon the alloy" [9]. The phenomenon of sensitization is now well known and it refers to the precipitation of metallic carbides and/or nitrides at the grain boundaries in a stainless steel or alloy, thus causing the alloy to be prone to intergranular corrosion or intergranular stress corrosion cracking.

Cihal et al. stated that chromium depletion occurs from the localized steel matrix which is adjacent to the grain boundaries. These chromium depleted zones causes precipitation of chromium rich carbides at the grain boundaries, which usually occurs in steel when solubility of carbon exceeded either due to prolonged exposure at elevated temperature range of 550-850°C or during slow cooling from temperature range of 1000-1200°C (solution annealing temperature range) [10]. A typical sensitized structure with carbide and/or nitride precipitates is shown in Figure 2.1. Peckner et al. stated that as chromium is the key element that determines the corrosion resistance of the steel, therefore the chromium depletion leads to the intergranular corrosion of the steel [11]. In stainless steel sensitization only occurs when the carbon content surpasses the solubility limit and therefore the vulnerability to sensitization can be efficiently reduced by decreasing the carbon content of the steel. Since Strauss et al. and Bain et al. first

advanced the mechanism of sensitization, various chromium depletion models have been proposed [12]. Stawstrom et al. focused on the creation of chromium depleted zones and the kinetic features of the carbide growth. The temperature and the time required to sensitize and de-sensitize a 304 austenitic stainless steel can be calculated from their model on the basis of carbon content and grain size [13]. Fullman et al. predicted the effect of alloying elements such as chromium, nickel, carbon, molybdenum, nitrogen, manganese etc., on the tendency of the alloy to get sensitized [14]. Devine et al. stated that severe sensitization can occur with only 0.008 weight% carbon forming carbides and that the maximum inter carbide spacing controls the greatest degree of sensitization [15]. Significant precipitation leads to severe chromium depletion adjacent to the grain boundary. Intergranular degradation which includes intergranular stress corrosion cracking and intergranular corrosion occurs when a sensitized steel is exposed to corrosive environments [16]. Sensitized grain boundaries offer linked networks for degradation. Such degradations often limit the service life of austenitic stainless steel components. Various studies have reported measurements of chromium depletion at the grain boundaries and correlated it with the microstructure [17]. The energy and the structure of the grain boundary decide the degree of sensitization and morphology of the metallic carbide(s) precipitation [16-17].

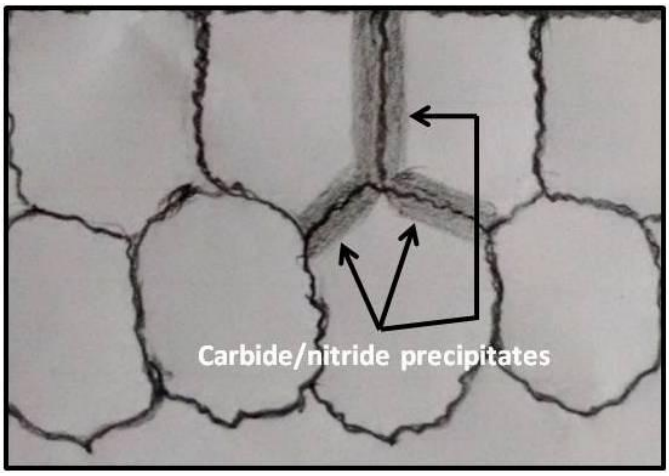

Fig 2.1: Precipitation of metallic carbides and/or nitrides at the grain boundaries

Watanabe introduced the concept of grain boundary engineering on the basis of concurrent lattice site model and it came forth to be a cheaper substitute to improvise properties like corrosion resistance of various materials which have low stacking fault energy [18]. Over past

two decades the subject of grain boundary engineering has evolved which aspires to improve the inter granular properties of materials having face centered structure by increase in special grain boundaries contributed during period of plentiful annealing twinning followed by thermo mechanical processing [19-21]. The reduction in grain boundary energy minimizes the effect of sensitization by increasing the lattice sites common to more than one grain. Grain boundary engineering has improved sensitization, intergranular stress corrosion cracking and intergranular corrosion cracking resistance and plasticity in austenitic stainless steels [21]. The grain boundary engineering process involves iterative deformation with application of low level of pre-strain followed by annealing at elevated temperature for longer duration of time.

Earlier researches on sensitization of various materials have divulged the nature of precipitation [22], the precipitation kinetics and the aging behavior [6] involved. It is established that the aging behavior can be judiciously illustrated from the time-temperature–sensitization diagram, as suggested by Dutta et al. [4]. Some studies indicate that sensitization of austenitic stainless steel contributes to the formation of martensite as a result of the deformation induced in them. Some detailed transmission electron microscopy (TEM) examinations on the characteristics of the precipitates have indicated that sensitization leads to the formation of chromium-rich $M_{23}C_6$ carbides, Cr-N, Cr_2N, and chi phase; the chi phase is a stable inter-metallic compound containing iron, chromium, and molybdenum of type $M_{18}C$ [23]. In addition to the studies related to the precipitates, some studies indicate that sensitization can lead to the formation of martensite as it happens by deformation in 304 austenitic stainless steels. Shankar et al. have studied the consequence of sensitization on tensile properties whereas Hilders et al. studied the effect on the toughness behavior of 304L austenitic stainless steel. The deterioration in ductility has been explained by Shankar et al. [24] and Hilders et al. [25] in terms of the precipitation of Cr-N, Cr_2N, and chi phase, the interaction of these phases with the dislocations, and the associated stress build up at the grain boundaries. The fall in toughness of the sensitized 304L austenitic stainless steel was determined on the basis of dimple size measured from the tensile fractographs. Tavares et al. reported the drop in the toughness value of the sensitized 304L steel through the Charpy impact test. The authors ascribed that this decrease in the toughness value was due to the fractional transformation of austenite to martensite which induces strain [6]. Ghosh et al. reported that the increase in deterioration of ductility and fracture toughness of the

AISI 304LN grade stainless steel with an increase in the degree of sensitization has already been established while studies reveal that degree of sensitization have almost no effect on the values of the tensile strength of the steel specimens. The author have reported that there is significant amount of triaxial stresses present within the grains and abundant growth of voids together result in transgranular fracture that occurs with a slight deformation in the sensitized samples [6].

2.3 Fatigue-Basic conceptions

Fatigue in metals has long been related with the variations in stress and strain. 150 years ago Wöhler discovered the fact that led to the development of the rotating bending machine. The rotating bending machine has been efficiently used throughout these years to derive an understanding of the phenomenon of fatigue and to characterize the fatigue resistance of various materials. It is usually established that cyclical plastic deformation is the fundamental and crucial factor in the growth of cumulative damage that takes place during cyclical loading. The cyclical plastic deformation all through the whole volume of the loaded metal changes the mechanical properties [26]. Localized cyclical deformation is the basic requirement for the formation of micro-cracks at the nucleation sites, and the rate of the cyclical deformation in the plastic zone to the fore of the crack tip determines the behavior of fatigue macro-cracks. Knowledge of the laws regularizing the fatigue process is very vital from various points of view. It permits to choose the processing treatment resulting in better fatigue resistance, yields the input data for the material classification, and forms the base for quantitative models of cumulative damage [27].

On the basis of the irreparable changes caused by the cyclical deformation, the fatigue process is divided into three partially overlapping stages:

a) Fatigue softening and/or hardening taking place as a result of the interaction involving structural defects mainly dislocations in the complete loaded volume. The behavior of

fatigue softening/hardening depends on the preliminary condition of the material and on the parameters of cyclical loading like mean stress, stress amplitude, temperature, etc.

b) Nucleation of the fatigue cracks resulting from the localization of cyclical plastic deformation at nucleation sites.

c) Propagation of the cracks which is governed by the cyclical plastic deformation localized in the plastic zone [28].

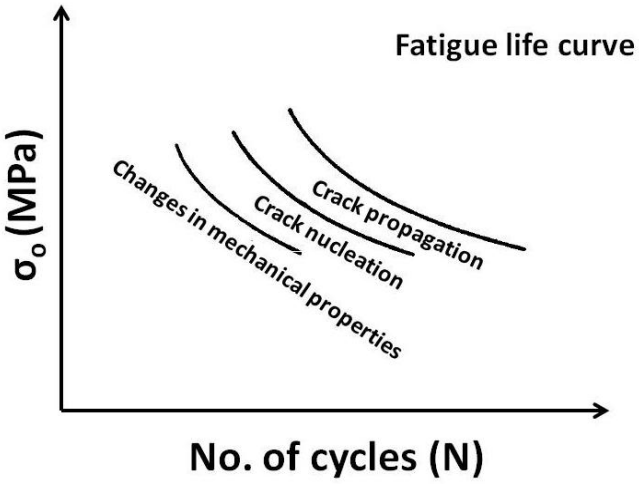

Fig 2.2: Stages of fatigue life of a component

Figure 2.2 represents the various stages of the fatigue process. The three curves represents the end of the softening/hardening stage, end of the crack nucleation stage and the end of fatigue crack propagation stage respectively and thus ending the complete fatigue process. In the nonexistence of major internal flaws such as large inclusions, the fatigue cracks generally initiate at the surface of the specimen and their preliminary growth is usually in the direction of the maximum shear stress. The more expected sites for a crack initiation are pre-existing highly stressed areas for instance notches, pits and scratches, or surface notch-like valleys, large inclusions on the surface and discontinuities ensuing from a slip along the crystallographic planes [29].

2.3.1 Factors affecting fatigue life

Fatigue life of a component is affected by various factors and they are microstructural details of the material such as grain size, texture; pre-history such as pre-loading, manufacturing process; load spectrum for instance sign, magnitude, rate, history; environmental conditions such as temperature, corrosive medium; and geometry of a component for example surface finish, notches, welds, connections, thickness. The figure 2.3 depicts a block diagram of the factors affecting fatigue life. From the diagram it can be inferred that sensitization occurs as a result of corrosive environment and that it has detrimental effect on the fatigue life of a specimen [29].

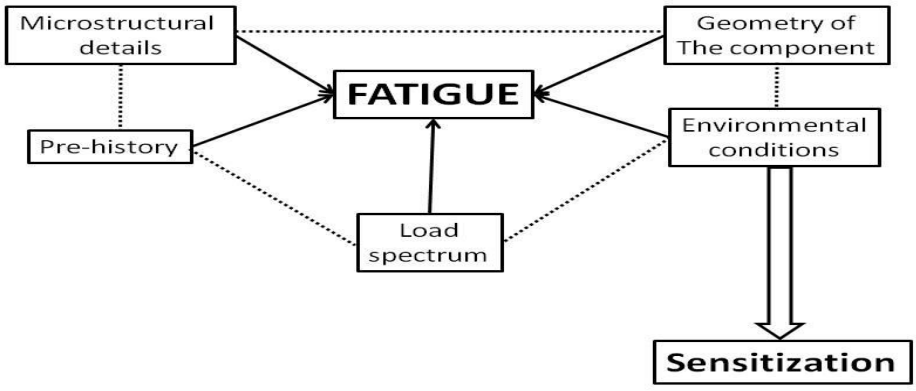

Fig. 2.3: Factors affecting fatigue life of a component

2.3.2 Types of load applications

The various types of variable loading that may cause fatigue in a component during its working life are shown in figure 2.4.

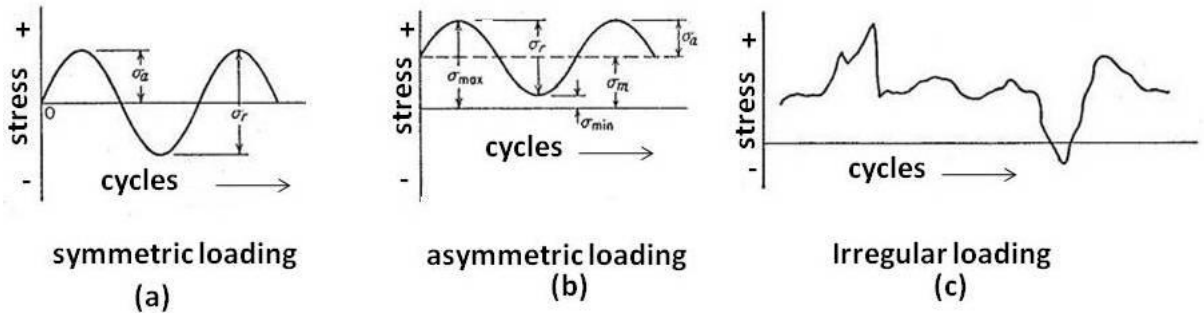

Fig. 2.4: Types of loading imposed on a component

Figure 2.4(a) represents a completely reversed cycle of stress of sinusoidal form. This represents symmetric cyclical loading with mean stress value equal to zero. Here the value of maximum stress is equal to minimum stress. The tensile stress is considered positive whereas compressive stress negative. Figure 2.4(b) represents an asymmetric cyclical loading in which the value of maximum stress and minimum stress are not equal. The figure depicts both σ_{max} and σ_{min} in tension. However, in a repeated stress cycle or asymmetric cyclical loading both the maximum and minimum stress could be of opposite signs or both in tension or compression. Figure 2.4(c) represents an irregular and random cycle where the component might be subjected to periodic unpredictable loading as in aircraft wings due to gusts [29].

2.3.3 High cycle fatigue and low cycle fatigue

High cycle fatigue is the fatigue condition in which the number of cycles to failure is greater than 10^5 cycles and if the number of cycles to failure is less than 10^4-10^5 cycles then the fatigue condition is called low cycle fatigue. To be more appropriate high cycle fatigue is related with pure elastic behavior of the component however low cycle fatigue is associated with plastic behavior of the material. High cycle fatigue is usually stress controlled and involves low amplitude and high frequencies. Figure 2.5(a) represents a typical S-N curve where maximum stress(S) is plotted as a function of number of cycles to failure (N). The figure depicts the nature of S-N curve for both ferrous as well as non-ferrous materials. From the figure it is clear that there is a particular well defined value of fatigue/endurance limit for ferrous materials which is not well defined in case of non-ferrous alloys [27].

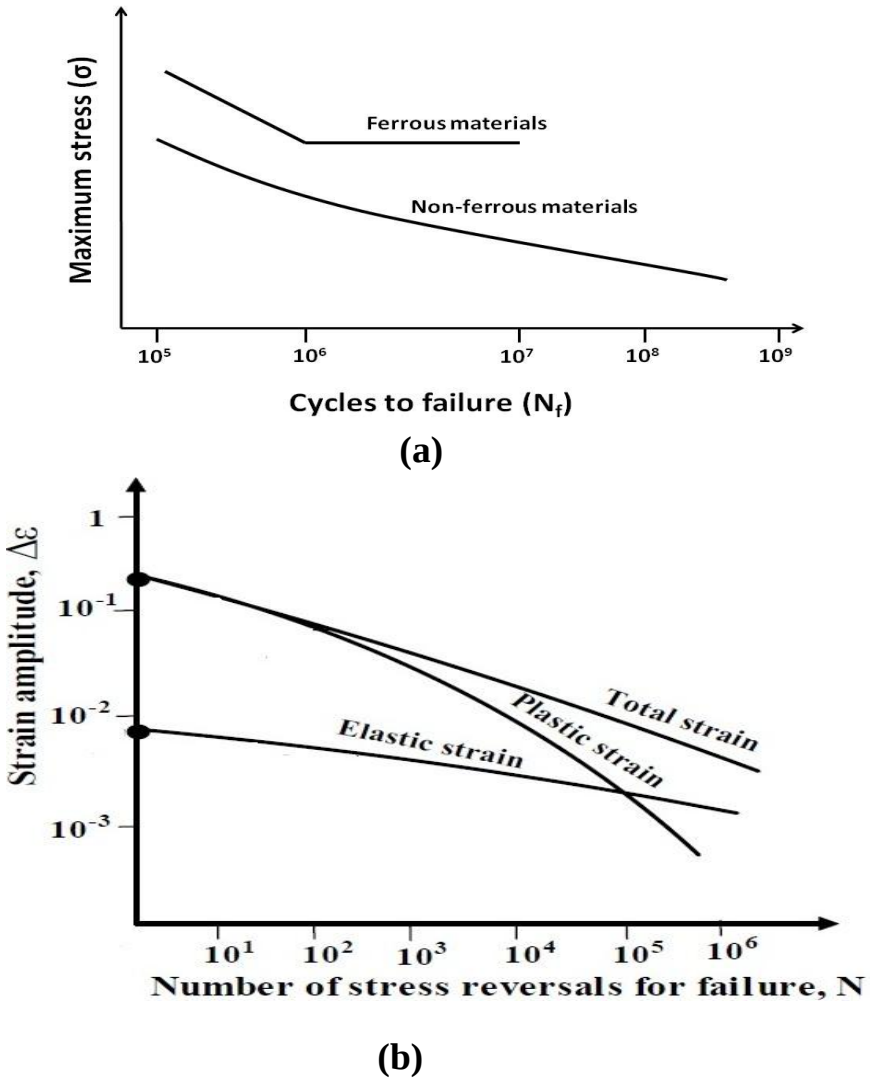

Fig. 2.5(a): Maximum stress(S) versus number of cycles to failure (N) curve and **(b):** plot of strain amplitude versus number of stress reversal cycles for failure

A low cycle fatigue failure usually begins at a localized discontinuity when the stress at that point surpasses the elastic limit. Then there is plastic strain which is responsible for crack propagation, crack growth and fracture. Low cycle fatigue is investigated in terms of cyclic strain. Figure 2.5(b) represents typical stain amplitude versus no. of stress reversals to failure plot for steel. Though strain controlled low cycle fatigue phenomenon is more common still stress controlled low cycle fatigue is also encountered.

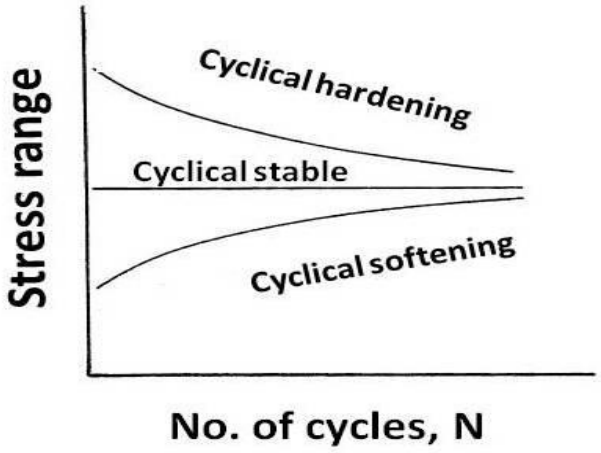

Fig 2.6: plot of cyclic hardening/softening behavior in low cycle fatigue

The shapes of hysteresis loops are variable throughout the fatigue life of all the materials and this change depends on the hardening/softening behavior of the material. A typical plot of cyclic hardening/softening behavior in low cycle fatigue is shown in Figure 2.6. From the figure it is clear that increase in stress amplitude with increasing number of cycles represents cyclic hardening whereas decrease in stress amplitude value represents cyclic softening [27]. However the stress amplitude value changes only in initial phases of fatigue life and then remains constant depicting stabilization of cyclic stress strain response of the material.

2.3.4 Cyclical Hardening/softening process

Cyclical loading of the metals and alloys result in change in their microstructure and properties. The intensity of the changes gradually decreases to zero with continuous increase in the number of the cycles thus indicating the end of the first stage of the fatigue process. The relation between stress and strain within one cycle is represented by a hysteresis loop. Figure 2.7 represents a typical hysteresis loop. Fatigue tests can be either stress controlled or strain controlled. There is a change in both shape and area of the hysteresis loop during cyclical hardening/softening process [29].

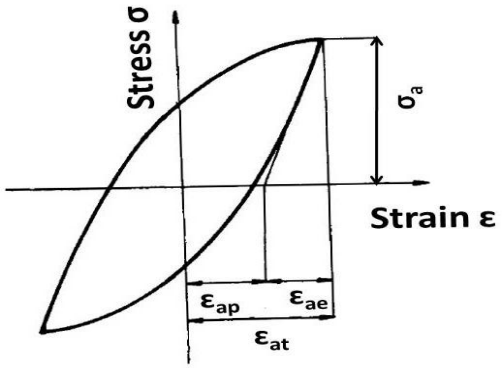

Fig 2.7: Schematic representation of a fatigue hysteresis loop. Here, Stress amplitude is denoted by σ_a, total strain amplitude ε_{at}, plastic and elastic strain amplitudes ε_{ap} and ε_{ae}, respectively.

Cyclic hardening in a plastic strain amplitude controlled tests is characterized by increase in both total strain amplitude and stress amplitude. When the polycrystalline copper is cycled at different total strain amplitudes, the stress amplitude is found to increase quickly at the beginning of cycling and attains a more or less ideal saturated value in a fraction of the total number of cycles to fracture. Cyclical hardening occurs typically in annealed materials. Whereas cyclical softening generally occurs in materials hardened either by cold-working, or by precipitates or by solute atoms. However in certain materials like low carbon steels and interstitial iron alloys, the fatigue process initially consists of hardening process which subsequently changes to softening process with increase in the number of cycles. Certain materials even exhibit no clear saturation which implies that microstructural changes of the total structure takes place from the commencement of the cycles till the complete failure. The hardening/softening curves depend on temperature and strain rate (i.e. frequency of cycling). The higher the frequency and the lower the temperature, the higher will be the saturated stress amplitude for the given plastic strain amplitude. This holds both for bcc metals and for fee metals [27-29].

2.3.5 Material reaction to cyclical loading

The stress strain relationship of a material depends on diverse factors such as environmental conditions, loading rate, temperature etc. When the specimen is subjected to one of the loading processes as shown in Figure 2.8, the response will vary depending on the mode of controlled

variable. The vital characteristics include cyclic mean stress relaxation, cyclical creep deformation and cyclical hardening/softening process. If the experiments are strain-control then the response could be cyclic hardening/softening. However if mean stress is present then there may be mean stress relaxation. For strain-hardenable materials the plastic strain decreases with the increase in the number of cycles and attains a stable state and the reverse occurs for strain-softenable materials. There will be additional accumulation of strain because of the presence of non-zero mean stress, in each loading cycle. This phenomenon is commonly known as ratcheting but has also been referred as cyclic creep or cyclic creep strain by a few investigators [26-29].

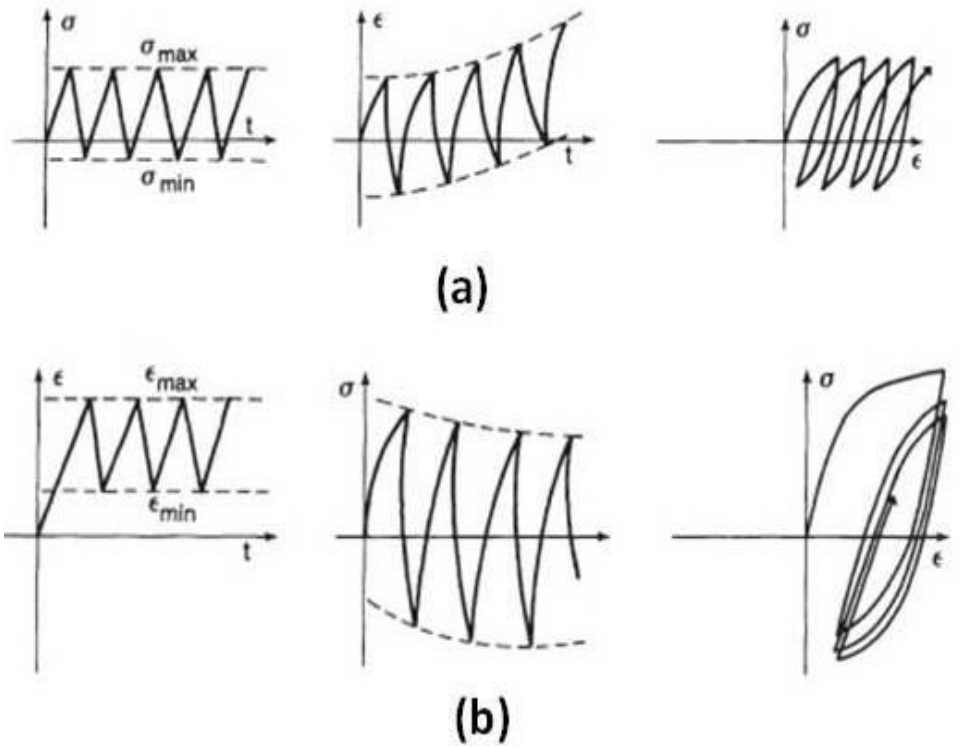

Fig 2.8: Plots of response of material subjected to cyclic loading. (a) cyclic creep and (b) mean stress relaxation.

2.4 Ratcheting

Low cycle fatigue is usually strain controlled. However stress controlled low cycle fatigue under asymmetric cyclical loading is known as ratcheting. Conventionally ratcheting is known as cyclical creep as this is a stress controlled fatigue test for prolonged duration of time [30]. Further effects of cyclic stresses are dependent on the temperature of the test [31]. Ratcheting can be defined as occurrences of continuous accruement of inelastic strain when a material is subjected to cyclical loading characterized by non-zero mean stress. Hysteresis loops produced by ratcheting deformation shifts towards higher plastic strain direction with increase in number of cycles [29].

Ratcheting is defined as progressive accumulation of plastic strain. Plastic strain accumulates within the material till the material's ductility exhausts and rupture takes place. The rate of ratcheting strain accumulation decreases with increasing number of cycles and the material attains a steady state [32]. Ratcheting strain can be mathematically calculated as the average of maximum and minimum strain. It can be expressed as

$$\mathcal{E}_r = (\mathcal{E}_{max} + \mathcal{E}_{min})/2 \qquad (2.7)$$

Where, $\mathcal{E}_r$ = *axial ratcheting strain*

$\mathcal{E}_{max}$ = *maximum strain at a particular cycle*

$\mathcal{E}_{min}$ = *minimum strain at that cycle.*

Ratcheting-fatigue phenomenon plays a very crucial role in design of load bearing structural parts which may be subjected to asymmetric loading during their service life. The earliest works available in literature are of Kujawski et al. [32] and Yoshida et al. [34] that addressed ratcheting response of various materials as the number of stress cycles increased. Later on, Yoshida et al. [35] put forward a uniaxial ratcheting model used to calculate ratcheting strain on the basis of biaxial stress cycles using equivalent ratcheting strain. However the model was extremely dependent on stress ratio, maximum stresses and several coefficients obtained experimentally. Rider et al. [36] examined the influence of ratcheting on the life of components using two steel alloys En3 and En19 subjugated to axial and torsional stress cycles. The authors described that the shear strain life curves are affected by the materials ratcheting behavior under torsional

cycles on the basis of Manson equation. Kang et al. [37] reported the effect of axial mean stress on the values of ratcheting strain calculated from the tests performed with zero mean shear stress under axial torsional loading conditions [38].

Various investigators studied the ratcheting behavior of various materials like SA 516 Gr. 70 steel [39], AISI type 304 stainless steel [40], SA 333 Gr. 6 steel [39] and carbon steel. Kulkarni et al. investigated the biaxial and uniaxial ratcheting deformation of SA 333 Gr.6 steel at room temperature [41]. For a pipe subjected to constant internal pressure and cyclical bending load it was observed that ratcheting deformation occurred in circumferential direction with no ratcheting strain in longitudinal direction. The ratcheting rate reduces with increase in number of cycles but increases with increase in load levels. Gupta et al. studied the ratcheting fatigue failure of pressurized low carbon manganese steel elbows and established that mean stress and ratcheting strain has significant effect on the low cycle fatigue life of a component. Xia et al. stated that both the tensile mean stress and ratcheting strain have damaging effects on the life of the component [42]. Kang et al. performed a number of uniaxial ratcheting tests on 304 austenitic stainless steel to study the cyclical strain characteristics, ratcheting and failure behavior. The authors discussed the results of stress mean and stress amplitude on ratcheting behavior of a material under uniaxial asymmetric cyclical loading. The material depicted cyclic hardening due to the strain amplitude. The ratcheting strain rate also decreased with increase in the number of cycles because of the materials cyclic hardening behavior [37-40].

Kang et al. and Hassan et al. have reported that plastic strain gets accumulated in the presence of positive or negative value of mean stress [40,43]. The authors stated that with increase in the value of mean stress the accumulation of ratcheting strain decreased. Kulkarni et al. reported that with increase in strain level the value of ratcheting strain and therefore the rate of ratcheting strain increases [41]. For lead tin solder the value of ratcheting strain increased with increasing mean stress for constant value of stress amplitude [44]. Lim et al. described that ratcheting strain accumulation is positive for positive values of mean stress and for negative mean stress the strain value is negative. Chen et al. stated that value of ratcheting strain rate and strain amplitude for 63Sn37Pb increase with increasing value of mean stress as well as stress amplitude [44]. Feaugas and Gaudin [45] reported that for 316 austenitic stainless steel, the ratcheting strain accumulation increases with increase in the value of mean stress at constant value of mean stress. Kang et al.

reported that when the value of stress ratio is -1, no ratcheting is noted as the stress cycling becomes symmetric. The author reported that for stress ratio of -0.714 maximum value of ratcheting strain was recorded which further decreased with increase in the values of stress ratio [31].

2.5 Re-assessment of the recent problem

It is by now clear that austenitic stainless steels are prone to sensitization when exposed to a temperature range of 550°C - 850°C thus making them vulnerable to intergranular corrosion. Austenitic stainless steels are used as pipelines for steam transfer in nuclear power sectors and in chemical industries where there is a chance of getting sensitized. These pipelines may also be exposed to cyclical loading which may or may not be symmetric. Hence always there is a chance of ratcheting deformation along with sensitization effect. To the best knowledge of the current investigator, no work exists in literature delineating the combined effect of ratcheting and sensitization of stainless steel. Therefore, the current investigation aims to study the effect of ratcheting on the mechanical properties and fatigue life of a sensitized austenitic stainless steel.

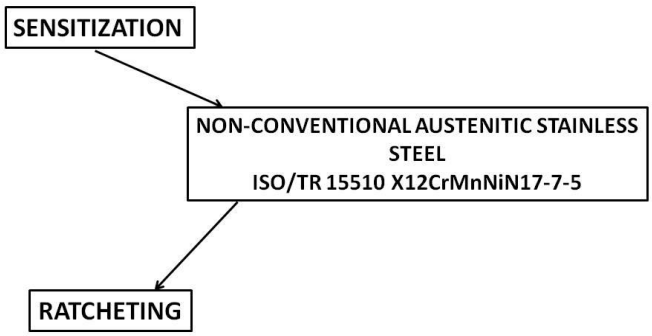

CHAPTER 3

Experimental details

3.1 Introduction

It is known that ratcheting is a special kind of low cycle fatigue deformation and thus this phenomenon got considerable interest of the scientific community throughout the globe. In last two decades, various materials have been studied for their ratcheting behavior, butt as perv the current knowledge of the investigator the ratcheting behavior of non-conventional austenitic stainless steel under sensitization has not been reported. Therefore the present research aims to study the effect of sensitization on mechanical properties and ratcheting behavior of non-conventional steel. The essential necessities prior to the ratcheting behavior examination of the selected stainless steel are the information concerning the microstructural and conventional mechanical properties such as hardness and tensile behavior.

Therefore the list of experiments conducted are summarized as determining the chemical composition of the chosen steel, imparting solution annealing heat treatment and thermal sensitization, determining their hardness, tensile properties and ratcheting.

3.2 Experimental procedures

In this segment, the diverse experimentations that have been carried out to fulfill the objectives are described.

3.2.1 Material, chemical analysis and heat treatment

A special grade of non conventional austenitic stainless steel denominated as X12CrMnNiN17-7-5 accordant with ISO/TR 15510:1997 [46] was used for the investigation. The commercially pure stainless steel was available in the form of 16mm diameter rods. The chemical composition

of the selected material was assessed using optical emission spectrometer (model: ARL 3460 Metals Analyzer, Thermo Electron Corporation Limited, Switzerland).

The pre deformation record of the chosen stainless steel is unknown. Hence it is indispensable to eliminate any residual stresses present. To do so solution annealing heat treatment was imparted to the selected material. Solution annealing restores the material to its initial condition, withdrawing alloy segregation, sensitisation and restoring ductility after cold working. The various heat treatment processes imposed on the selected stainless steel are:-

i. Solution treatment of the non conventional stainless steel by soaking at *1050°C* for *1 hour* followed by water quenching.
ii. Thermal sensitization of the steel at 750°C with ~~a~~ soaking periods of
    a. *Five hours*
    b. *Ten hours*
    c. *Fifteen hours*

All these treatments were followed by rapid water quenching.

3.2.2 Microstructural analysis

Samples of approximately 10 mm height were cut from the various heat treated rods for metallographic examinations. These samples were ground approximately on a belt grinder. After rough grinding, samples were polished using a series of emery papers of grades of 1/0, 2/0, 3/0 and at last 4/0. They were moved in perpendicular direction to the existing scratches during each polishing operation. These were then polished in cloth polishers, first using alundum and finally using 0.25 µm diamond paste. In addition to that, the solution annealed stainless steel samples were electro polished using a solution of 20% perchloric acid and 80% acetic acid in ice-cooled atmosphere at a current density of 25 A/dm^2 for 5-15 minutes. The polished specimens were etched with freshly prepared aqua regia solution ($3HCl:1HNO_3$) for 8 seconds.
Microstructure of the samples were obtained by optical microscope (Model: ZEISS AxioCam ERc5s), and images were captured at different magnifications. Optical microscope has been shown in Figure 3.1.

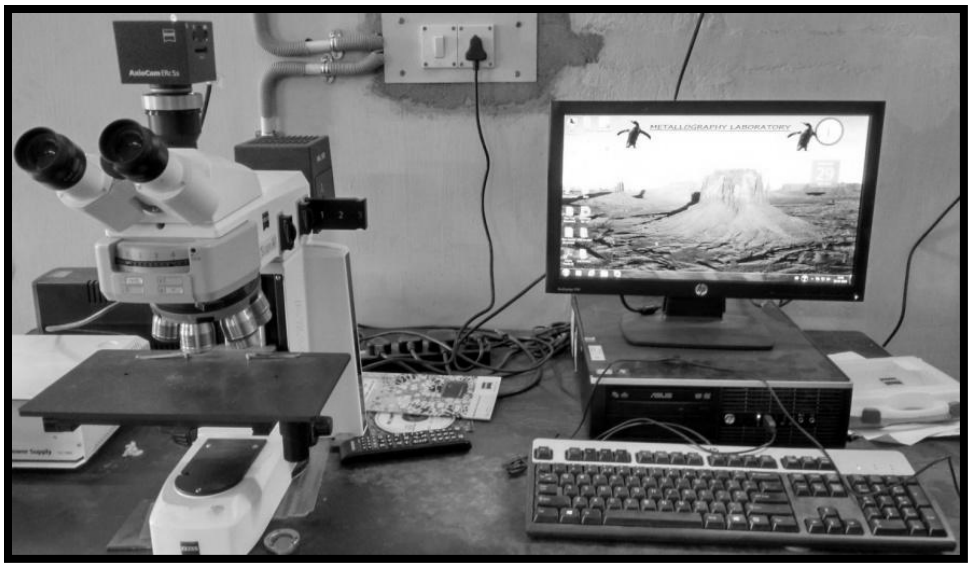

Fig. 3.1: Image of optical microscope

The average grain size was approximated using linear intercept method following ASTM standard E-112 (2013). In this process, a linear test grid was superimposed on the microstructure and the number of intercepted grains with the test line was counted carefully. Such measurements were repeated at least on 300 grains. The grain size (d) was calculated as:

$$d = \frac{L_T}{N_L} \tag{3.1}$$

Where,

N_L = number of grains intercepted by a unit true test line length.

L_T = true length of the test line which can be defined as the length of the test line at unit magnification.

The microstructural characterization of the sensitized samples were done using scanning electron microscope (Model: JEOL-JSM 6480LV) for better understanding. Corresponding energy dispersive x-ray spectroscopy (EDS) analysis was also done both at the grain boundary as well as throughout the matrix to get a quantitative assessment of the composition of the components. A typical scanning electron microscope is shown in figure 3.2.

Fig. 3.2: Image of Scanning electron microscope (SEM)

3.2.3 Hardness measurement

The samples prepared for microstructural analysis were further used for determination of hardness values. Hardness values were measured using a Vickers microhardness tester LECO LV 700, Michigan, USA. Microhardness values of the non-conventional stainless steel have been taken at different positions of the sample. Dwell time for microhardness test is 10 sec, with applied load of 25gf. The hardness of the sensitized steel specimen was measured both within the grain as well as at the grain boundary and compared with the solution annealed stainless steel specimen. The Vickers microhardness tester machine is shown in figure 3.3.

Fig.3.3: Image of Leco LV 700 Vickers Microhardness Tester

3.2.4 Tensile properties measurement

Cylindrical samples having 6 mm gauge diameter and 25 mm gauge length following ASTM standard E8M-09 (2009) were prepared for tensile tests. All the tests were done at room temperature. The tests were done using a universal testing machine (Instron 1195, Birmingham, UK) at 1 mm/min cross head speed and this speed corresponds to nominal strain rate of 6.66×10^{-4} s^{-1}. For each test the load and displacement values were recorded and were used to prepare load versus displacement graphs. A typical configuration of a tensile sample is shown in figure 3.4

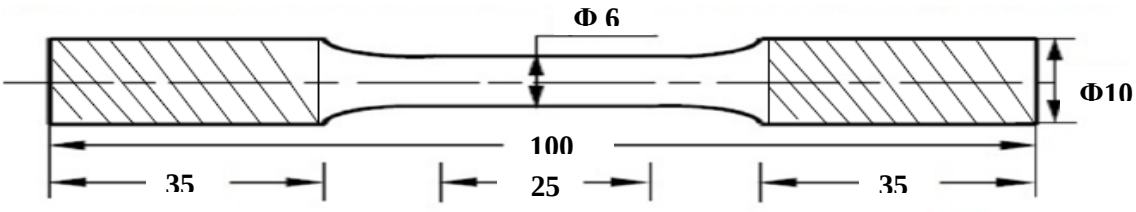

Fig 3.4: Sample design for tensile test

3.2.5 Fatigue properties determination

The heat treated rods were machined to fabricate fatigue samples having gauge length and diameter of 15 mm and 7 mm respectively as per ASTM E606. The lower length to diameter ratio for the fatigue specimens is to accommodate simultaneous tensile and compressive strains properly; the specimens get buckled for any higher length to diameter ratio. Stress controlled low cycle fatigue tests were carried out using ±100 kN universal testing machine (Model: BISS UTM, Bangalore, India). All the tests were done at room temperature at a constant stress rate of 50 MPa/s and for 150 cycles. Keeping the stress mean constant, the stress amplitude was varied for every 50 cycles as shown in fig.3.6. Details of the stress parameters are listed in Table 1. For each test, at least 200 data points for every cycle was tried to obtain and stress and strain values were calculated with the help of the software MTL32 provided with the machine.

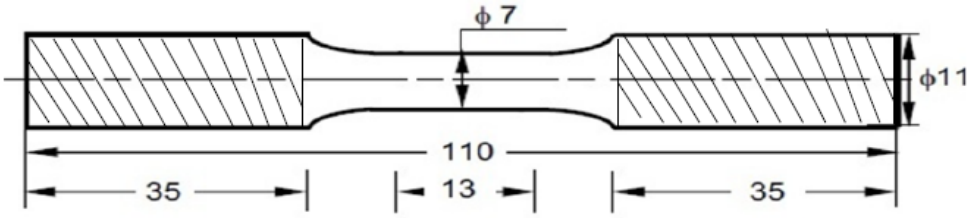

Fig 3.5: Sample design for fatigue test

Table 1: Stress parameter values for stress controlled low cycle fatigue tests

Heat Treatment Condition	**σ_m (MPa)**	**σ_a (MPa)**
Solution Annealed	30	200
		240
		270
Sensitized 05 hours	30	200
		240
		270
Sensitized 10 hours	30	200
		240
		270
Sensitized 15 hours	30	200
		240
		270

All the ratcheting tests were done for 50 cycles for each value of stress amplitude to procure better results.

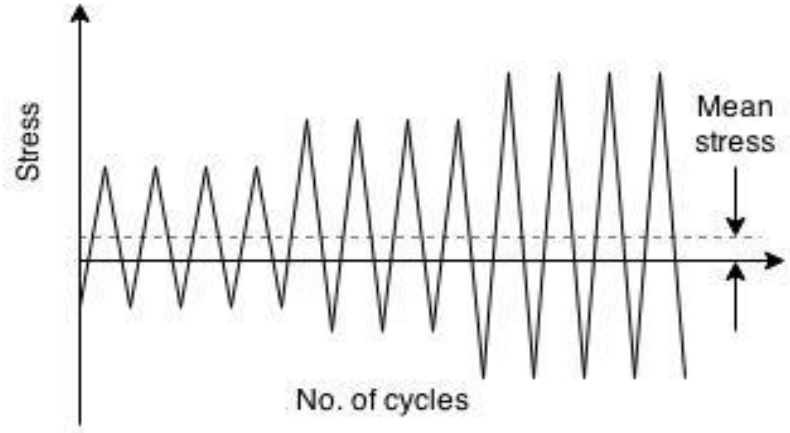

Fig 3.6: Loading history of stepped uniaxial asymmetric stress cycles with constant mean stress

3.2.6 Post ratcheting tensile

To study the extent of cyclical deformation, the tensile properties of the ratcheted samples have been carried out. The tests were done in the same procedure as mentioned in section 3.24. The values of load and displacement were obtained to calculate corresponding stress strain values. The characteristic configuration of a broken post ratcheting tensile sample is given in Figure 3.7.

Fig. 3.7: Image of Broken post ratcheting tensile samples

3.2.7 Fractographic examination

The fractured surfaces from the broken tensile and post ratcheting tensile samples were carefully cut for fractographic examination. Transverse sections were cut from the broken gauge portion of the samples and were examined using the scanning electron microscope at various magnifications.

3.2.8 X-ray diffraction

To determine presence of any in situ microstructural variations, X-ray diffraction studies were carried out. Representative samples were analyzed using Cu-Kα radiation of a high-resolution X-ray diffractometer (Model RIGAKU JAPAN/ULTIMA-IV). The specimens were scanned to generate X-ray diffraction patterns in the 2θ range 40 –100°, with a step size of 0.05° and scan rate of 5°/min.

CHAPTER 4

Results and discussion

4.1 Introduction

In this section the results produced during characterization and study of fatigue behavior of the sensitized stainless steel are presented and discussed elaborately. As this investigation aims to study the ratcheting behavior of the sensitized non-conventional stainless steel therefore tensile and fatigue properties of both solution annealed and sensitized samples were estimated. Experiments were conducted as discussed in chapter three and the results obtained are discussed The sensitization heat treatment was imparted to the investigated steel for various time durations i.e., 5, 10 and 15 hours so that the impact of sensitization could be properly studied with increasing degree of sensitization. A correlation between the applied stress parameters, accumulated strain and residual fatigue life of pre-ratcheted low cycle fatigue specimens is intended to draw.

4.2 Material composition and microstructural analysis

The chemical composition of the investigated non-conventional stainless steel X12CrMnNiN17-7-5 is provided in Table 4.1. This non-conventional stainless steel is a special grade of stainless steel which was developed to conserve nickel. The 300 series stainless steel is having very low carbon content with common alloying elements of Ni and Cr at a range of 16-25% and 8-20% respectively. As the investigated stainless steel also contains Cr, Mn and Ni as alloying elements which are austenitic stabilizers therefore the crystal structure of this steel is fcc at room temperature i.e., this steel is austenitic at room temperature. However, this non-conventional stainless steel is having 0.14% carbon with major alloying elements Cr, Mn and Ni as 15.6%, 5.49% and 3.96% respectively and thus preserving nickel.

Table 4.1 Chemical composition of investigated materials (all in wt. %).

Material	Elements						
ISO/TR 15510X12CrMn NiN17-7-5	**C**	**Cr**	**Mn**	**Ni**	**Cu**	**Mo**	**V**
	0.14	**15.6**	**5.49**	**3.96**	**1.05**	**0.2**	**0.06**
	Ti	**Al**	**Si**	**N**	**S**	**P**	**Fe**
	0.02	**0.03**	**0.53**	**0.135**	**0.016**	**0.042**	**Bal.**

Typical optical microstructures of the investigated steel are illustrated in Figure 4.1. Figure 4.1(a) is one representative image of the solution annealed steel. This figure indicates presence of equiaxed multidirectional grains, as one can except for a solution annealed austenitic stainless steel. The optical microstructures of the steel subjected to sensitization operation for varying sensitization times (viz. 5, 10 and 15 hours) are shown in Figures 4.1 (b), (c) and (d) respectively. The figures of the sensitized steel specimens reveal that there is a loss in directionality of the grains. One can find presence of annealing twins in abundance in the solution annealed steel. However the amount of annealing twins decreased in the sensitized 5 hours sample and is totally absent in both sensitized 10 and 15 hours samples. The grain size of the solution annealed steel is 23.49±3.6 μm whereas that of the sensitized steel at 750°C for 5, 10 and 15 hours are 6.09±0.683 μm, 6.53±0.77 μm and 8.296±1.387 μm respectively as obtained from liner intercept method according to ASTM standard E-112.

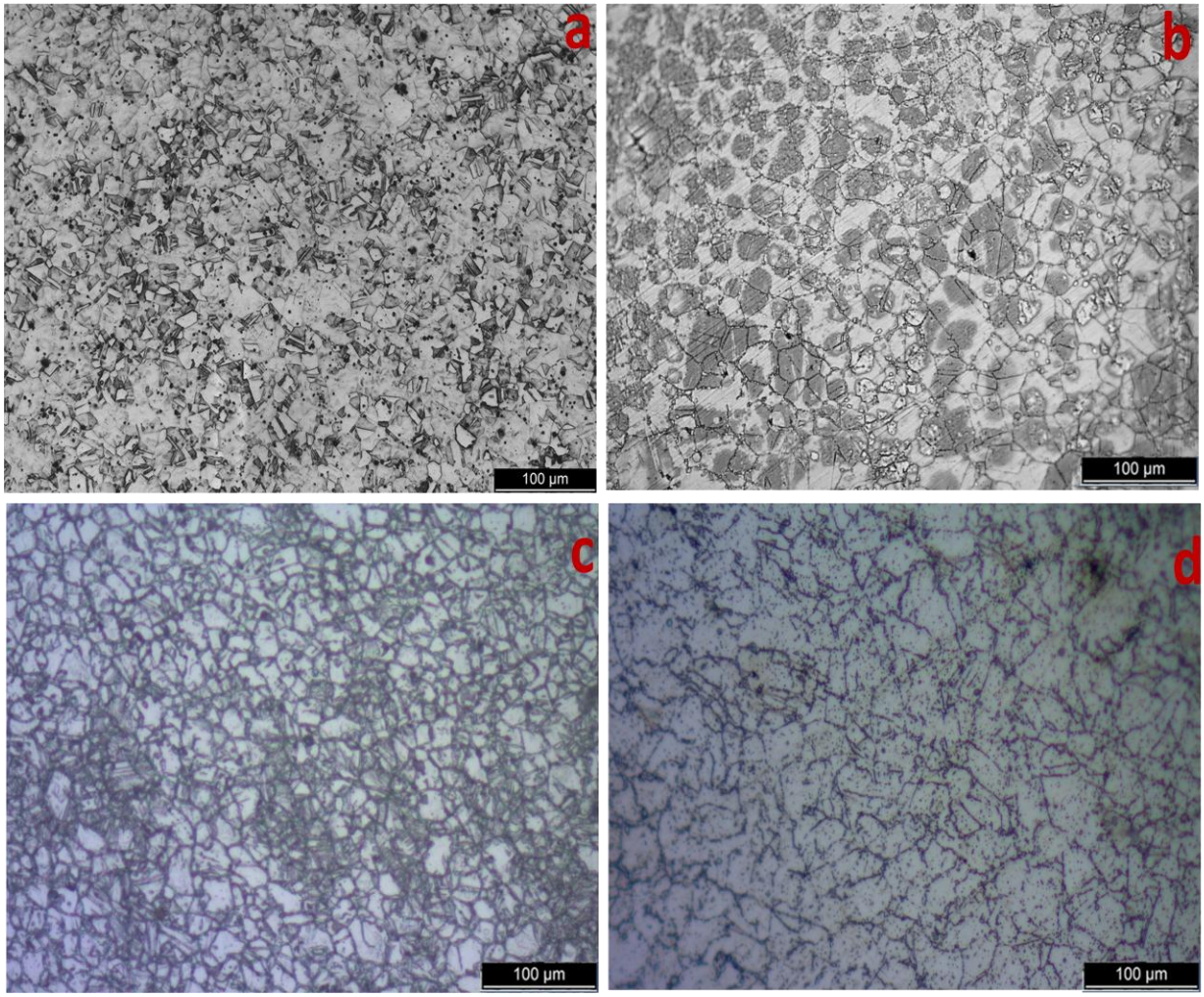

Fig 4.1- Micrographs of steel specimen at magnification 500X of (a) Solution annealed at 1050°C for 1 hour (b) Sensitized at 750°C for 5 hours (c) Sensitized at 750°C for 10 hours
(d) Sensitized for 750°C for 15 hours.

The scanning electron microscopy analysis of the sensitized stainless steel specimens were done to understand the effect of solute depletion. One representative figure of the sensitized 10 hours stainless steel sample is shown in Figure 4.2(a). One can note from the coloured x-ray mapping that concentration of chromium at the grain boundary region is more as compared to that in the grain interior. For better understanding, micrograph at higher magnification is taken and EDS analysis of a portion at the grain boundary is shown in Figure 4.2(b). However, this is a qualitative analysis. Hence, for quantitative assessment of Cr%, Table 4.2 and Table 4.3 are

given which indicates the weight % of various elements at the grain interior as well as the grain boundary.

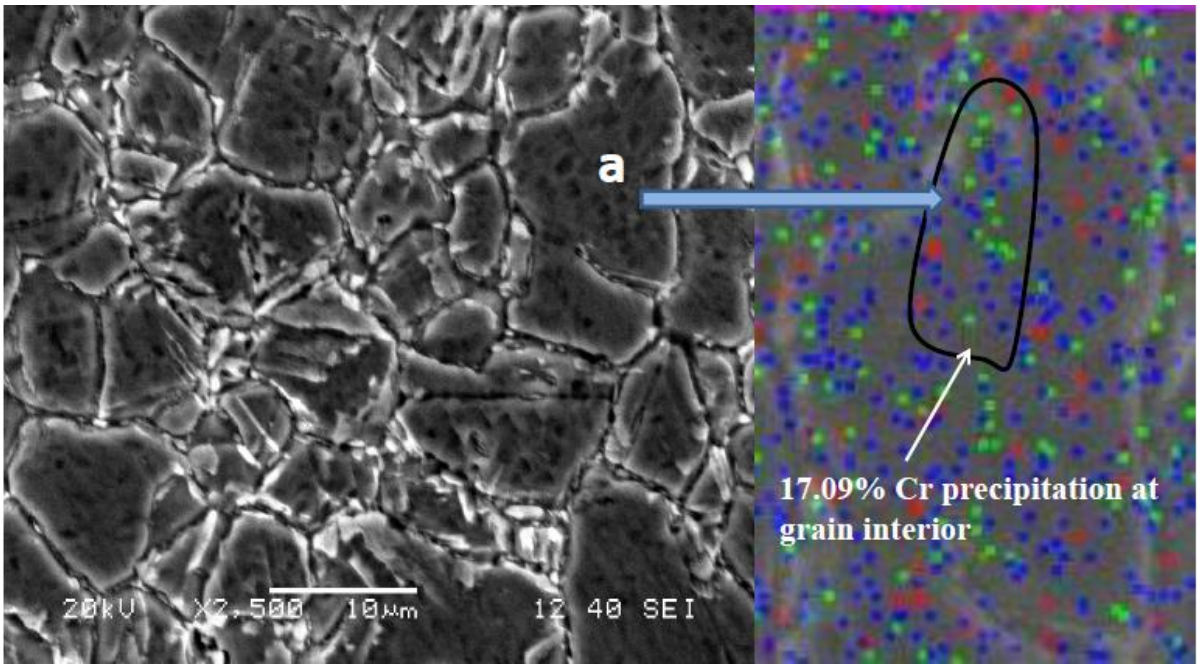

Fig 4.2(a): SEM image of the sensitized steel at 2500x magnification with corresponding EDS mapping of the grain marked (a).

The analysis of Cr% at the interior of the grain and at the grain boundary depicts that Cr% is more for the grain interior as compared to the grain boundary. The analysis of Cr% at the interior of the grain and at the grain boundary depicts that Cr% is more for the grain interior as compared to the grain boundary.

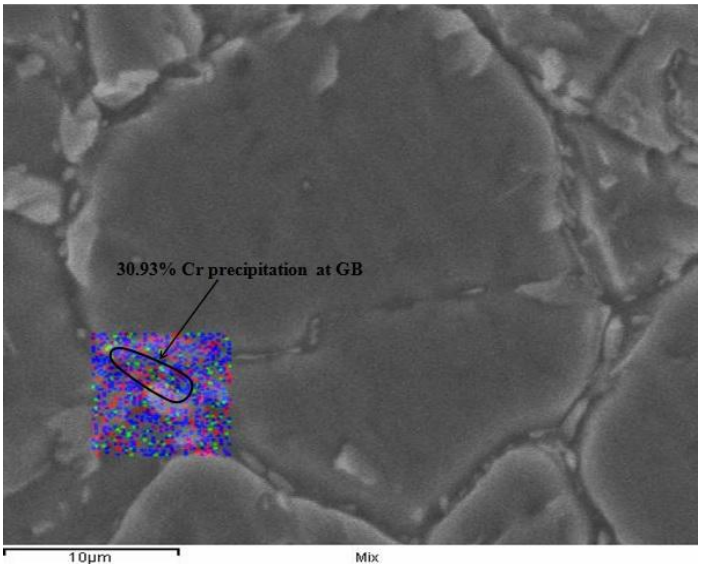

Fig 4.2(b): SEM image of the sensitized steel at 6500x magnification with corresponding EDS mapping.

Table 4.2: Chemical composition of the structure (overall)

Element	Weight %
Cr K	17.09
Mn K	6.02
Fe K	73.33
Ni K	3.66

Table 4.3: Chemical composition at the grain boundary

Element	Weight %
Cr K	30.93
Mn K	6.70
Fe K	62.37

In the EDS mappings the blue colour represents Iron (Fe), green represents Chromium (Cr), pink represents Manganese (Mn) and the purple represents Nickel (Ni).

4.3 Hardness determination

Hardness of the non-conventional stainless steel was taken at different positions of the samples. At least three readings were recorded for each case to calculate an average value of hardness. Dwell time of 10 seconds was used, with the applied load of 25 gf. The results are listed in Table 4.4.

Table 4.4: Microhardness values of the investigated non-conventional stainless steel

Heat treatment condition	**Hardness Value (Hv)**	
Solution annealed	326.4	
Sensitized	**Within the grain**	**On the grain boundary**
5 hrs	299.7	338.1
10 hrs	293.22	354.6
15 hrs	273.44	372.3

According to literature, the hardness value of the solution annealed non conventional steel is 213.86 $Hv_{0.050}$ measured at an applied load of 5 gf. However 25 gf load is applied in the current research. It is well known that Vickers hardness was calculated by using the relations:

$$H_V = 1.854P/(d_{avg})^2 \quad (4.1)$$

Where

P= applied load in kgf.

$d_{avg} = (d_1+d_2)/2$

Where, d_1 and d_2 are the lengths of two indentation diagonals. Therefore, as the value of load increased the hardness value increased. Ghosh et al. [6] reported decrease in hardness of 304LN stainless steel with increase in degree of sensitization. This is due to the depletion of solid solution strengtheners (Cr, C, Ni etc.) from within the matrix and precipitation in the form of metallic carbides and/or nitrides on the grain boundaries. It is clear from the table that the hardness values of the grain boundaries is more as compared to within the grain structure and also from that of the solution annealed matrix.

4.4 Tensile properties

Cylindrical samples were used to study the tensile properties of the inquired austenitic stainless steel as per the meticulous procedures mentioned in section 3.2.5. Figure 4.3(a) shows typical engineering stress strain graphs of all the heat treated conditions. The acquired data were examined to calculate the values of yield strength (YS), ultimate tensile strength (UTS), % uniform elongation (%ε_u), % total elongation (%ε_t), strain hardening exponent (n) and strength coefficient (k) of each heat treated condition. Figures 4.3(b) and 4.3(c), (d), (e) and (f) depict the true stress strain plot and further log (true stress) vs. log (true strain) in the plastic domain of solution annealed, sensitized 5, 10 and 15 hours respectively. The material at each heat treated conditioned have shown continuous yielding behavior from elastic to plastic region and hence their yield strength values have been estimated by 0.2% strain off-set procedure, as per suggestion given in ASTM standard E8M-08 (2008). Estimated total elongation values were cross checked with the ones obtained directly from the change in the gauge marks on the specimens after the test. Table 4.3 summarizes the average tensile parameters calculated for each condition.

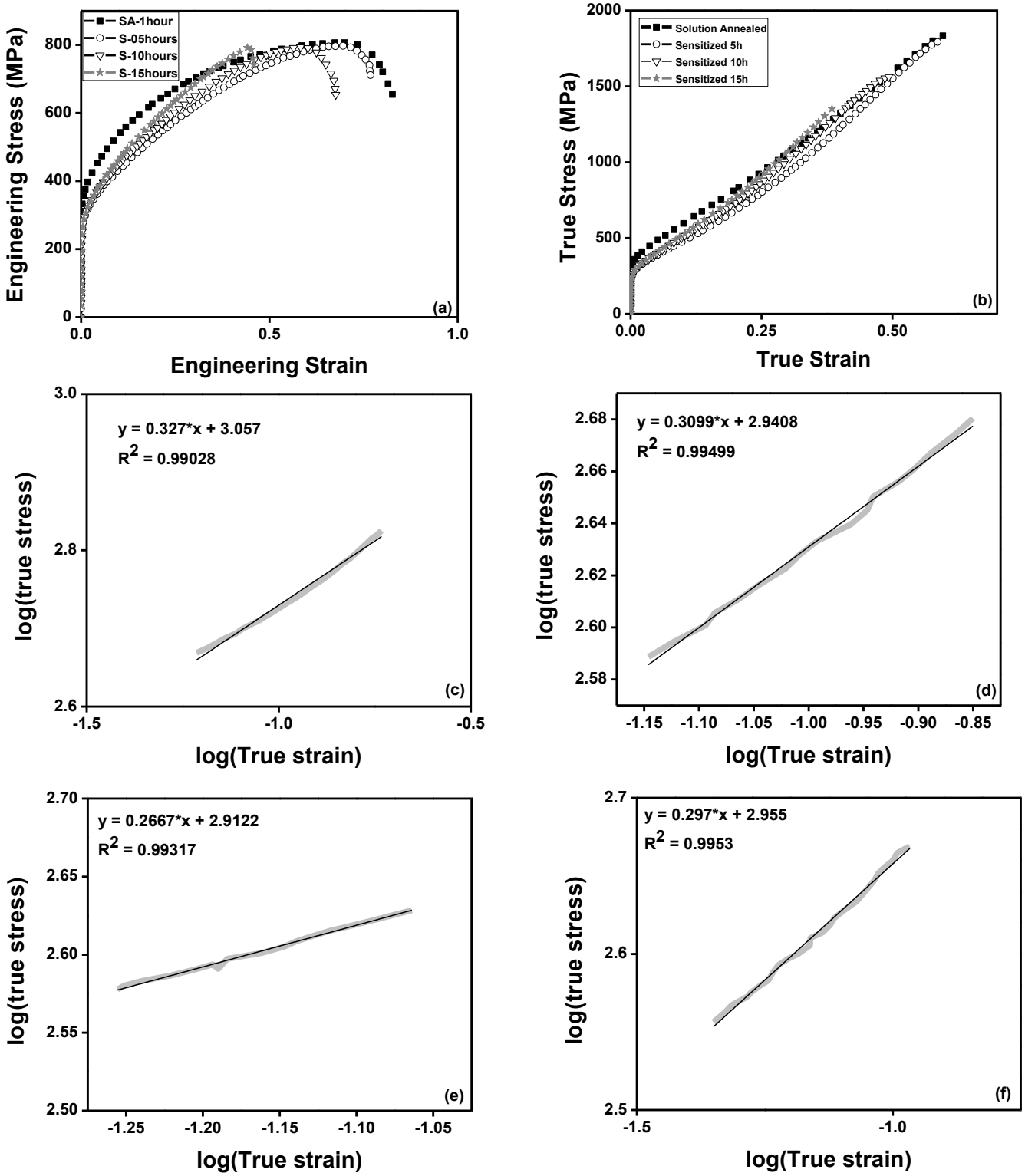

Fig. 4.3: (a) Engineering stress strain curve (b) True stress strain graph and (c), (d), (e) and (f) log (true stress) vs. log (true strain) in the plastic domain of solution annealed, sensitized 5, sensitized 10 and sensitized 15 hours respectively.

Table 4.5: Average tensile properties of the investigated material for different heat treated conditions.

Material condition	Yield Strength (MPa)	Tensile strength (MPa)	Uniform elongation % (e_u)	Total elongation % (e_t)	Strain hardening exponent (n)	Strength coefficient (MPa)
Solution Annealed	411	815	71	83.2	0.33	1140
Sensitized 05 hrs	242	797	69.9	76.8	0.31	873
Sensitized 10 hrs	225	794	57.8	67.9	0.27	817
Sensitized 15 hrs	169.8	793	45	45.8	0.29	901

It is clear from Figure 4.3 (a) that there is marginal decrease in TS however there is significant decrease in YS. The precipitation of metallic carbides and/or nitrides at the grain boundaries results in decrease in the solid solution strengtheners from the austenitic grain matrix with increase in degree of sensitization, thus decreasing YS. The drop in the value of YS may also be due to the fact that martensitic transformation occurs with increasing degree of sensitization. These factors also lead to decrease in the value of TS. However TS drop has been compensated by martensitic transformation and dislocation multiplication occurred during plastic tensile deformation [47]. Hence one can notice here direct effect of martensitic transformation.

Strain hardening exponent (*n*) values were calculated using Hollomon equation $\sigma=K\varepsilon^n$, where K is strength coefficient [48]. The values of strain hardening exponent, *n* have been calculated from the log-log plot, whereas strength coefficient, K is calculated from the intercept of this plot to the stress axis at $\varepsilon=1$. The values of *n* are found to decrease with increase in degree of sensitization. This may be due to the fact that martensitic transformation which is itself a hard phase restricts the hardening process.

Fractographic studies of the broken sample after tensile test was done using scanning electron microscope. Figures 4.4 (a), (b), (c) and (d) depict the fracture surfaces of the solution annealed and sensitized 5, 10 and 15 hours samples respectively.

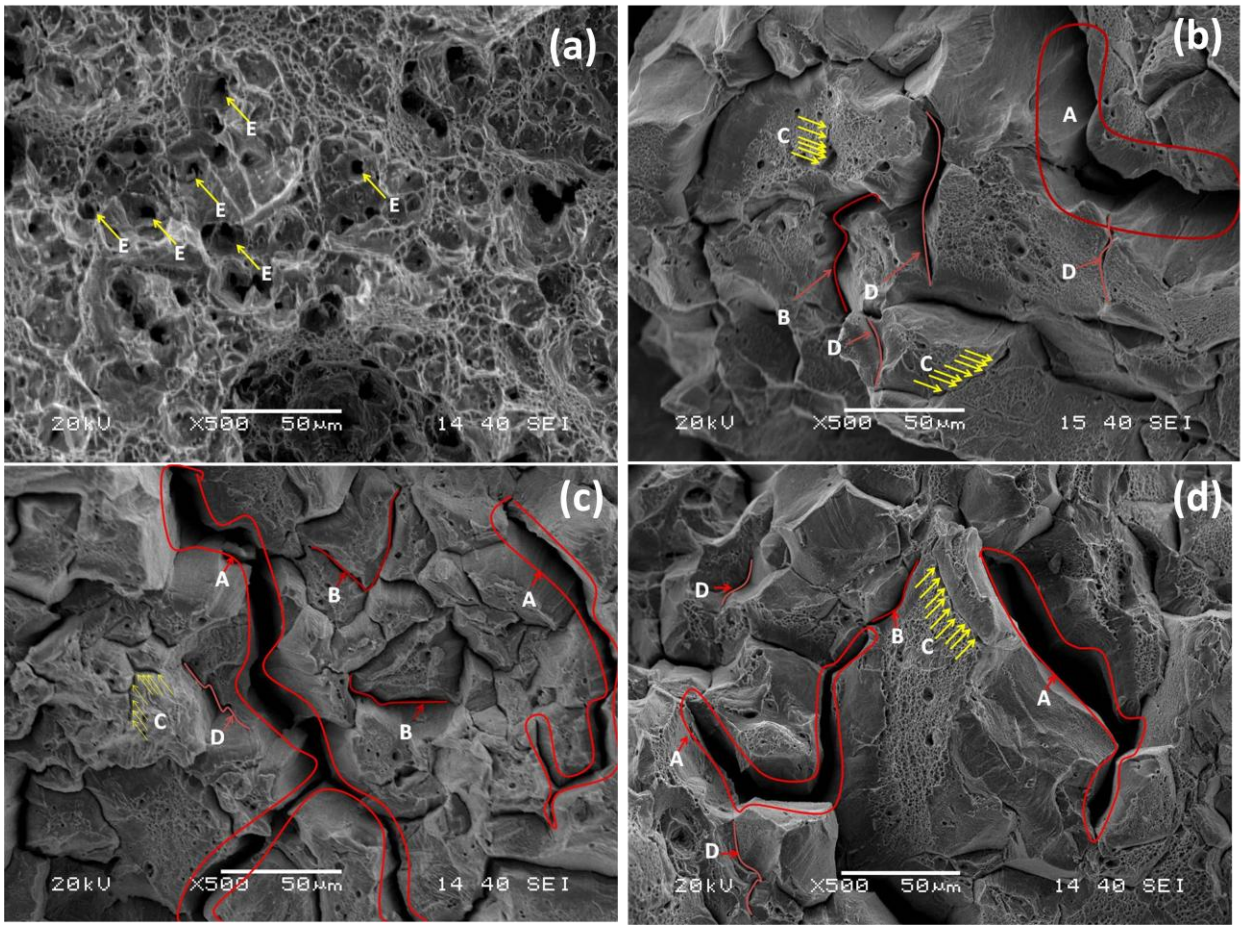

Fig.4.4: Tensile fractographs of non-conventional stainless steel at different heat treatment condition (a) solution annealed,(b),(c) and (d) are sensitized 5, 10 and 15 hours samples respectively. In these fractographs (A)-Intergranular fracture, (B) intergranular cracks, (C) aligned micro-ductility and (D) transgranular fracture are observed.

The solution annealed structure reveals dimple structure as expected for a ductile material like stainless steel. It is known that the mechanism of ductile fracture is made up of three successive effects- void nucleation, growth and their coalescences [49-50]. On analyzing the fracture surface of solution annealed specimen, it is concluded that the nucleation of voids in X12CrMnNiN17-7-5 austenitic stainless steel is created by inclusion matrix de-cohesion and/or dislocation-dislocation interaction. However for sensitized specimens, de-cohesion between the particle and the interface occurred at the grain boundary due to the solute precipitation. It is well known that intergranular corrosion cracking occurs in sensitized specimens due to precipitation of metallic carbides and/or nitrides which causes embrittlement of grain boundary. The fracture surface of the sensitized steel carries the signature of sensitization in terms of grain boundary

cracking. Ghosh et.al have reported that there is significant amount of triaxial stresses present within the grains and abundant growth of voids together result in transgranular fracture that occurs with a slight deformation in the sensitized samples. Similar kind of transgranular fracture is present in the fractographic images of the sensitized steels. However in sensitized samples the tendency for void formation is more at the grain boundaries and these combines to form grain boundary or intergranular cracks. It can be noticed that with the increase in degree of sensitization the amount of intergranular cracks increases and thus decrease in the transgranular cracks.

4.5 Uniaxial ratcheting behavior

The results of ratcheting tests conducted for different duration of cycles under different combinations of mean stress and stress amplitude have been incorporated and subsequently discussed in this section. Cyclic stress-strain hysteresis loops were generated from the uniaxial ratcheting experiments on the investigated material under different positive mean stress values. It is known that asymmetric cyclic loading with non-zero mean stress produces unclosed hysteresis loops. A typical hysteresis loop for the sensitized 5 hours sample is shown in Figure 4.5.

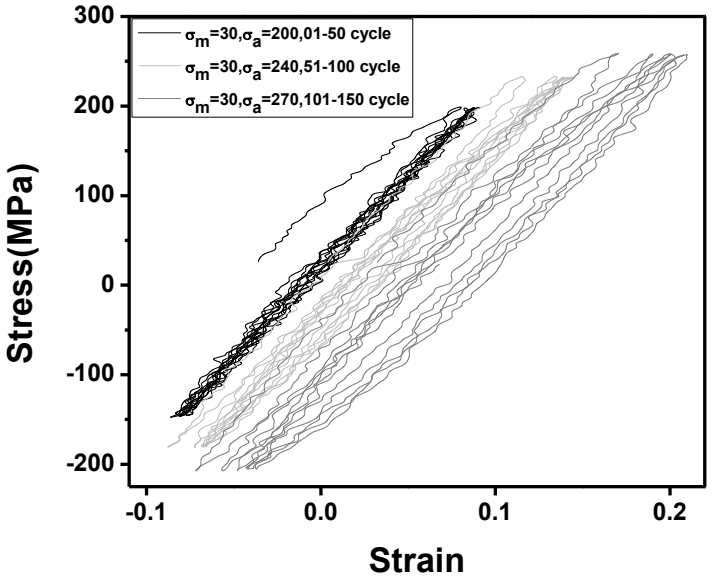

Fig.4.5: Typical hysteresis loops for the sensitized 5 hours sample.

The value of stress amplitude was varied for each 50 cycles. The variation of ratcheting strain (ε_r) with number of cycles for varying σ_a = 200, 240 270 MPa at constant σ_m = 30 MPa is examined. A typical plot of ε_r vs. N for solution annealed and sensitized 5, 10 and 15 hours steel is shown in Figure 4.6 respectively. The results indicate that ratcheting strain increases monotonically with increase in number of cycles for any σ_a -σ_m combination. It can be noticed that with increase in the value of σ_a for each 50 cycles the value of ratcheting strain rate increases. It can also be inferred that with increase in degree of sensitization the value of ε_r decreases. This may be due to increased amount of grain boundary segregation with sensitivity because it actually restricts the plastic deformation process and dislocation activity.

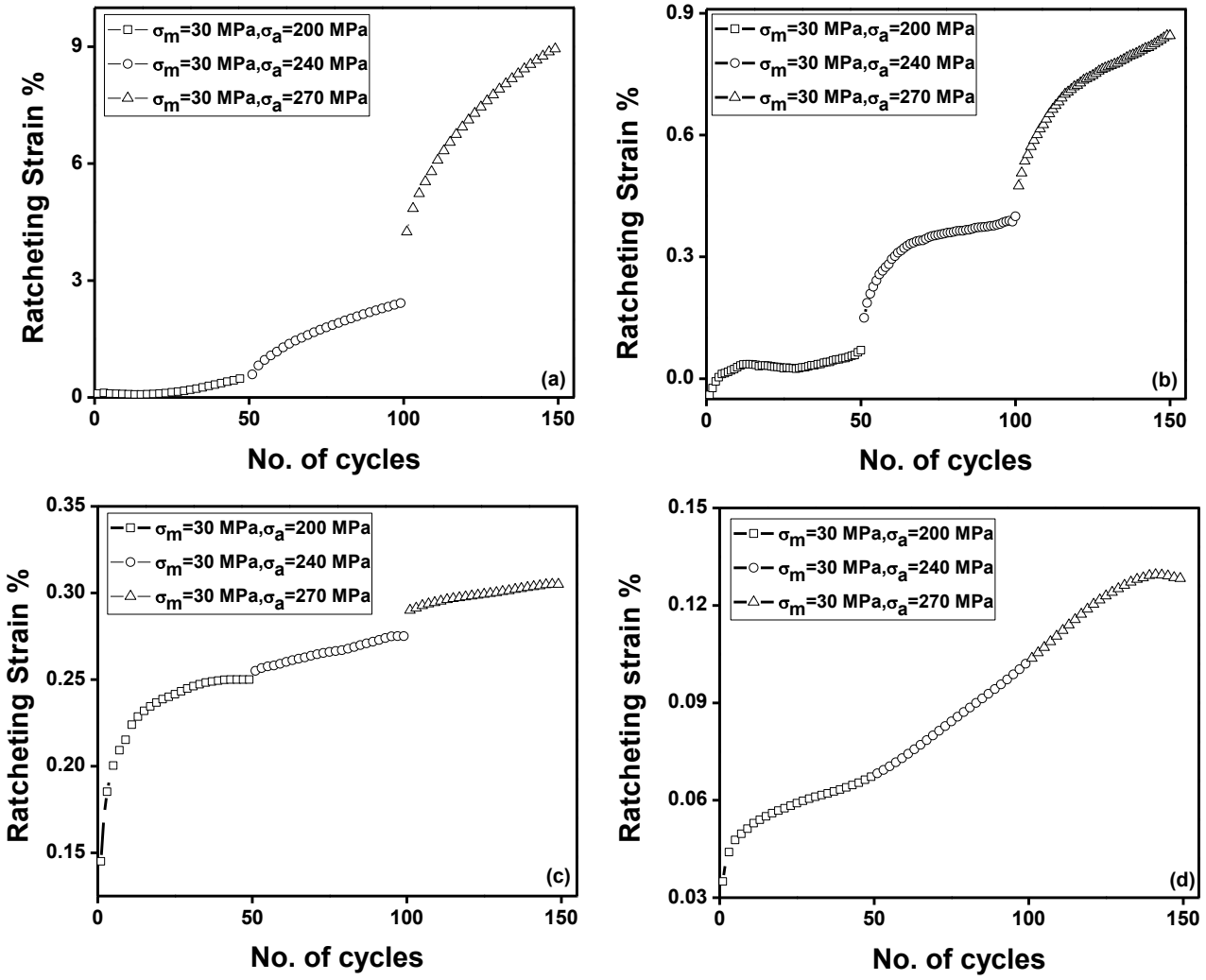

Fig.4.6: Typical plot of ε_r vs. N for (a) solution annealed, (b) sensitized for 5 hours, (c) sensitized 10 hours and (d) sensitized 15 hours.

4.6 Post-fatigue tensile properties

Tensile tests have been conducted on the same specimens which have been subjected to fatigue damage to study the tensile properties of investigated non-conventional stainless steel subjected to previous cyclic loading. Typical engineering stress-strain plots of the pre-fatigued solution annealed and sensitized stainless steel samples are shown in Fig.4.7 (a). One can note that although the variations in yield strength values do not follow any specific trend, the ultimate tensile strength values reduce as that compared with the ultimate tensile strength values of the specimens which have not undergone any previous fatigue cycling.

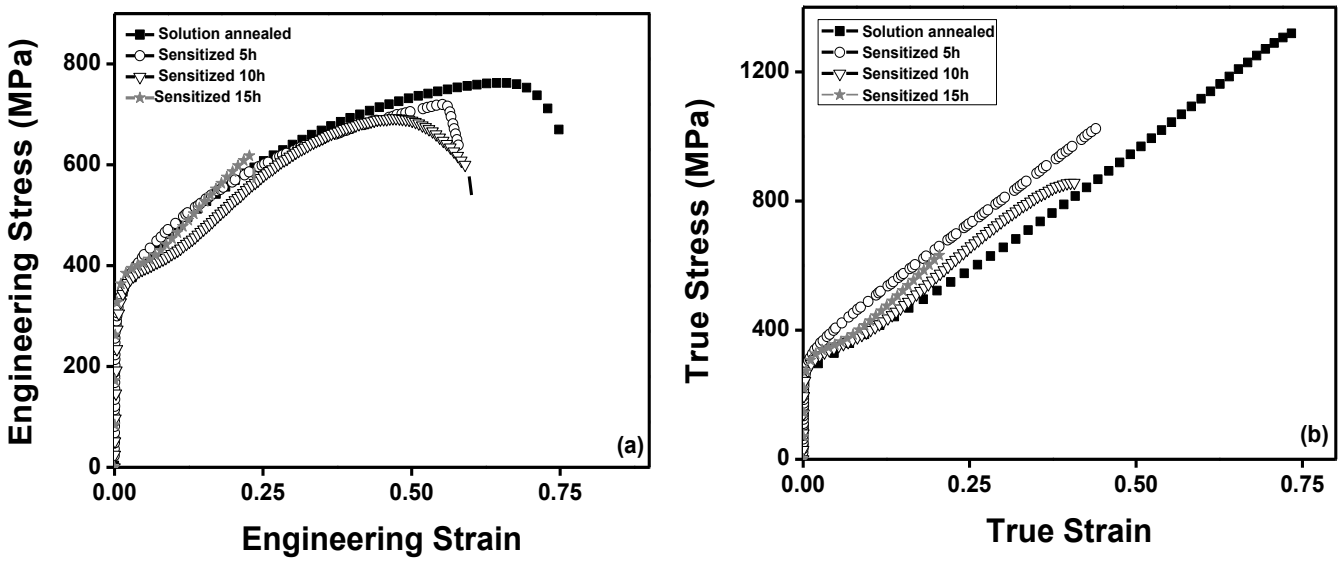

Fig. 4.7: (a) Engineering stress-strain plot of the post-fatigued solution annealed and sensitized stainless steel samples and (b) True stress strain plot of post ratcheting samples for different heat treated conditions.

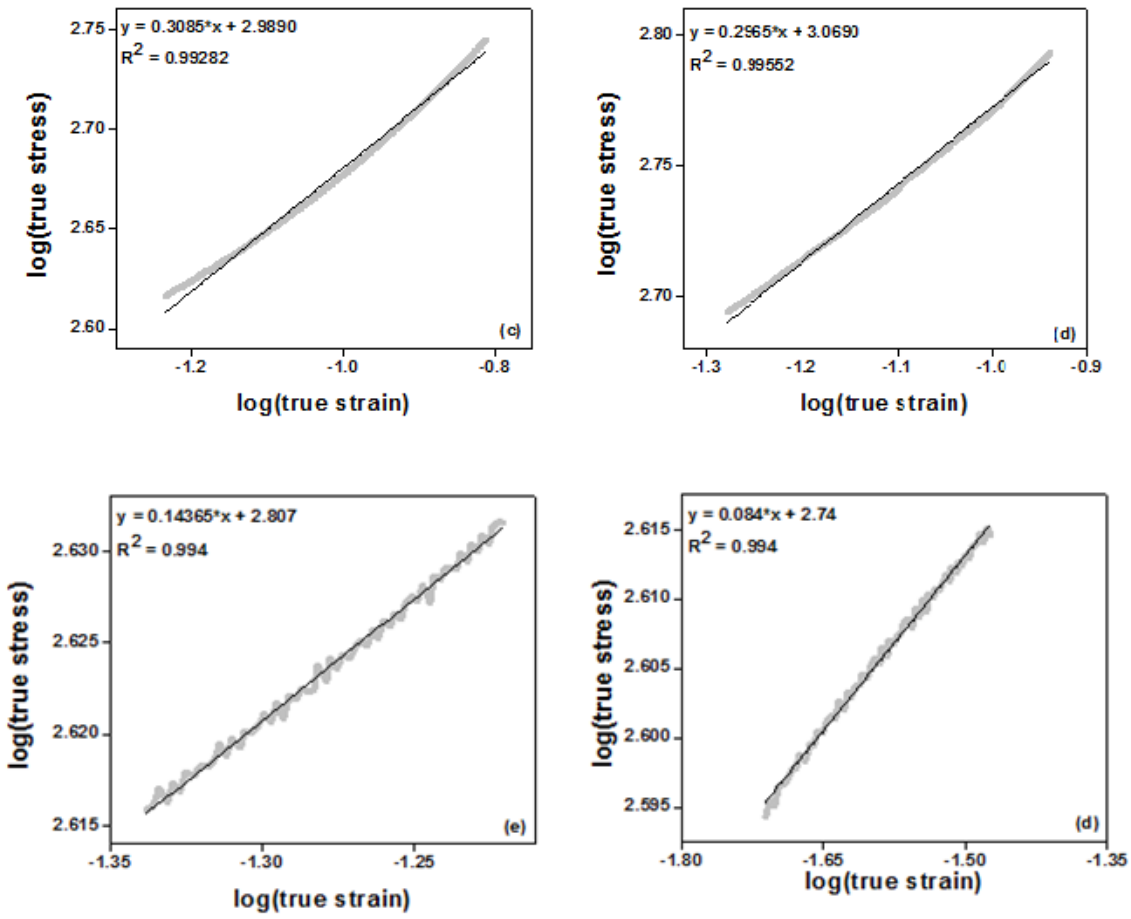

Fig 4.7 (c), (d), (e) and (f): log (true stress) versus log (true strain) plots of solution annealed, sensitized 5, sensitized 10 and sensitized 15 hours respectively.

Table 4.6: Tensile properties of the post ratcheted samples.

Material condition	**Yield Strength (MPa)**	**Tensile strength (MPa)**	**Uniform elongation % (e_u)**	**Total elongation % (e_t)**	**Strain hardening exponent (n)**	**Strength coefficient (MPa)**
Solution Annealed	347	763	65.41	76.6	0.31	975
Sensitized 05 hrs	369	720	55.78	57.9	0.30	1172
Sensitized 10 hrs	333	692	48.44	60.27	0.14	641
Sensitized 15 hrs	330	621	23	23.45	0.08	550

Figure 4.8(a) depicts fracture surface of a solution annealed sample subjected to stress jump ratcheting test for 150 cycles. The fracture surface of the broken tensile sample shows dimpled structure indicating ductile mode of fracture. A comparison of the fracture surfaces under unratcheted tensile and ratcheted tensile samples indicate that a few voids in the unratcheted sample has substantially grown up. This is reflected with the higher total elongation value of the unratcheted tensile specimen. Figure 4.8 (b), (c) and (d) represent the fracture surfaces (ratcheted + tensile) of the sensitized samples for 5, 10 and 15 hours respectively. These fracture surfaces indicate that the amount of rack candy fracture is more prominent with increase in degree of sensitization. However features attributing ductile dimples are also available, though the amount has decreased with increase in degree of sensitization. This can be correlated with the decrease in the strain values of post ratcheting tensile tests with respect to the corresponding strain values of tensile tests without ratcheting. It can be inferred that due to sensitization treatment, the ductility of the non-conventional stainless steel decreased.

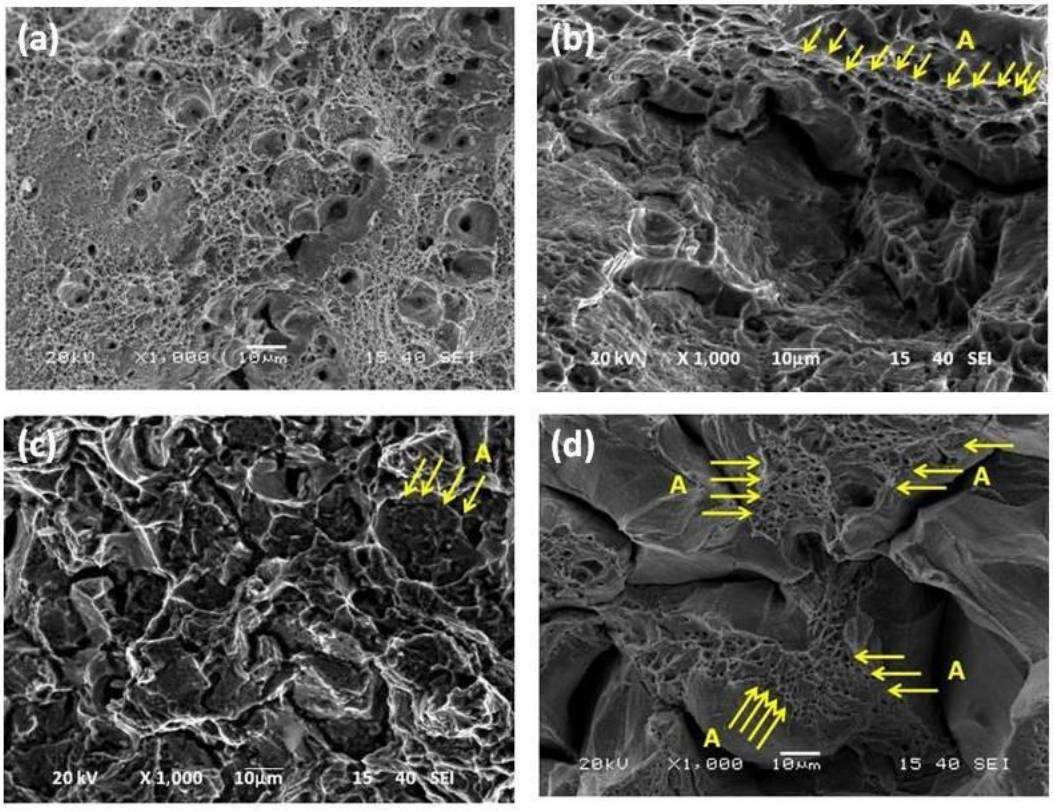

Fig.4.8: Post ratcheting fractographs of non-conventional stainless steel at different heat treatment condition (a) solution annealed, (b), (c) and (d) are sensitized 5, 10 and 15 hours samples respectively. In these fractographs (A) denotes dimpled structure

On comparing elongation values, one can note that for the sensitized 5 hours and 15 hours samples the difference between the values of uniform elongation and total elongation are very less. This is due to increase in the degree of sensitization which reduces the total plasticity of the material. A comparison of the tensile strength of unratcheted and ratcheted samples indicate that it reduces after ratcheting. Prior ratcheting deformation has softened the steel which is reflected in their tensile strength values. This softening feature can be noticed from the increment in the hysteresis loop area as clearly indicated in Figure 4.9. One can note that for the 2, 49, 52, 99, 102 and 149th cycles the loop area significantly increases with increase in number of cycles which indicate the softening of the steel upon cyclical loading.

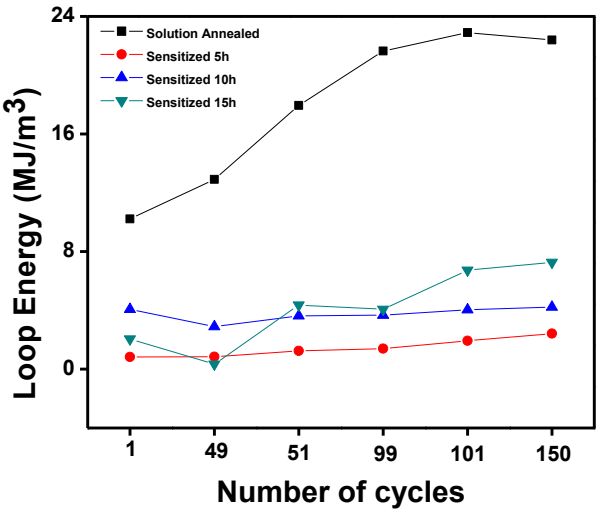

Fig 4.9: Plot of loop energy versus number of cycles.

4.7 In-situ variations of microstructure

It is known that the structure of austenitic stainless steels is metastable and according to its chemical composition, condition of thermomechanical treatment (deformation rate, temperature) etc., different kinds of phase transformations take place, such as $\gamma \rightarrow \varepsilon$, $\varepsilon \rightarrow \acute{\alpha}$, $\gamma \rightarrow \acute{\alpha}$, $\gamma \rightarrow \varepsilon \rightarrow \acute{\alpha}$. The volume percentage of the deformation generated phases has a great effect on the mechanical behavior and other properties (like corrosion) [50-51]. It is generally seen that by decreasing the working temperature, volume fraction of alpha martensite and epsilon martensite

increases while there is decrease in austenite. However, a few recent investigators reported that room temperature monotonic or cyclic loading may induce this kind of transformation, where both alpha and epsilon martensites form [50]. Kishor et al. and Dutta et al. suggested that ratcheting deformation produces considerable amount of strain-induced martensite [52-53].

Ghosh et al. has reported that martensitic transformation occurred in sensitized 304LN stainless steel. An attempt has been made in this investigation to study the martensitic transformation occurring in the sensitized non-conventional austenitic stainless steel during ratcheting. In view of this, X-ray diffraction studies of undeformed as well as deformed steels were done. Typical results in Figure 4.10 and 4.11 depict X-ray diffraction analyses for undeformed and deformed steels respectively. The results indicate that the undeformed steel in both solution annealed and sensitized condition doesn't have any martensitic peak (Figure 4.10). In comparison the steels which were deformed upto 150 cycles in stress jump tests show martensite transformation as confirmed by the presence of various alpha martensite (ά) peaks.

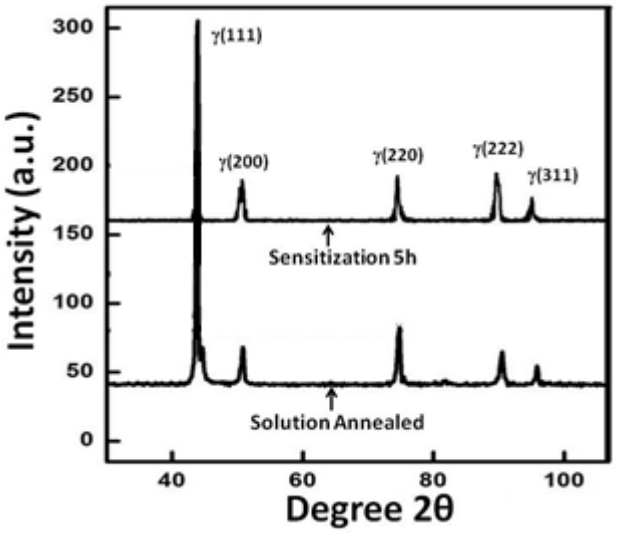

Fig 4.10: X-ray diffraction patterns of undeformed solution annealed and sensitized (5 hours) samples.

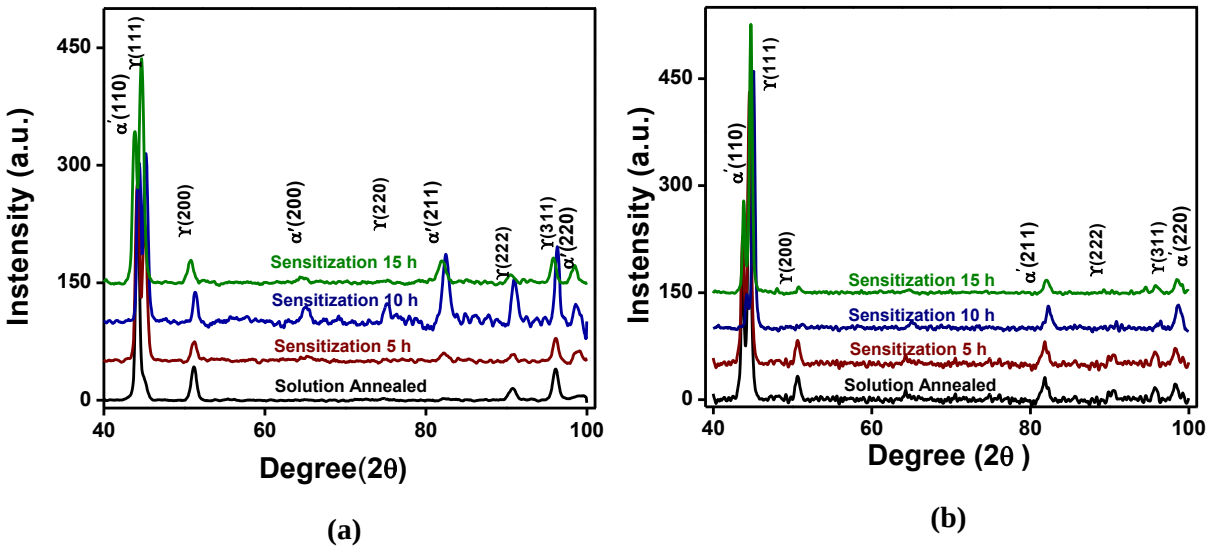

Fig 4.11: X-ray diffraction patterns of all samples after (a) tensile test (b) post ratcheting tensile test.

Yield strength of the material post ratcheting decreased because of the martensitic transformation prior ratcheting deformation of the material. Similar features have been noticed in the tensile strength of the material post ratcheting. Moreover the yield strength values of the samples decreased during tensile deformation with increase in degree of sensitization. All these are attributed to the formation of alpha martensite which is a hard phase. It is a known fact that martensitic transformation actually increases the strength of the steel. But due to sensitization the yield strength reduces with sensitization time. It was seen in section 4.4 that the variation in yield strength was a maximum of 58% whereas in section 4.6 the variation in yield strength was found to be only about 5%. This large reduction in the variation of yield strength value is attributed to prior martensitic deformation during ratcheting of the samples. Similar features can also be noticed for the variation of tensile strength.

Summarizing the effect of sensitization and combined effects of sensitization and ratcheting on the investigated non-conventional stainless steel, it can be deduced that the tensile strength and yield strength values of the material decreases with increase in sensitization time attributing to the fact that ductility of the non conventional steel reduces with sensitization. Ratcheting

deformation is found to increases with increase in stress amplitude values for constant values of stress mean. The yield strength and tensile strength value of post ratcheted steel samples were found to reduce. However, percentage reduction in tensile strength values of both ratcheted and unratcheted tensile samples was insignificant which is attributed to in-situ martensitic transformation during deformation, as also evidenced by X-ray diffraction profile analyses.

CHAPTER 5

Conclusions and future scope

Conclusions and scope for future research

5.1 Conclusions

The current investigation is dealt with ratcheting fatigue behavior of a non-conventional austenitic stainless steel. The obtained results and their pertinent discussion lead to the following conclusions:

1. In the solution annealed steel, presence of a plenty amount of annealing twins are observed. However the amount of annealing twins decreased in the sensitized 5 hours sample and is totally absent in both sensitized 10 and 15 hours samples. The amount of sensitized grain boundaries have increased in the sensitized steels. Yield strength decreases to a large extent while the tensile strength marginally decreases in the sensitized steel; the phenomenon is attributed to the transformation of austenite to deformation induced martensite in the steel.
2. Fractographic studies of the tensile samples indicate that intergranular fracture is the predominant fracture mechanism in the sensitized steel along with some transgranular fracture in the regions with classical ductile morphologies. However, fractographic studies of the sensitized post fatigue tensile samples indicate rock candy fracture as the prime fracture mechanism.
3. The accumulation of ratcheting strain increases with increasing stress amplitude. Stepwise increase in stress amplitude increases the rate of strain accumulation. However, the value of ratcheting strain decreases with increase in sensitization time. As ratcheting deformation occurs due to accumulation of plastic strain, strain accumulation decreases with increase in sensitization time as the brittleness of the material increases with sensitization.
4. The rate of ratcheting strain accumulation increases with step-wise increase in stress amplitude. This is attributed to the cyclic softening behavior of the material as confirmed by increase in the values of loop energy with increasing number of cycles.

5. The yield strength and tensile strength of the post ratcheted tensile samples decrease along with decrease in percentage total elongation values. This phenomenon occurs due to the in-situ martensitic transformation during prior ratcheting deformation as well as during tensile deformation of the material.

5.2 Scope for future work

The present study has generated some information regarding the fatigue and post-fatigue tensile behavior of a non-conventional stainless steel. A number of directions for future research can be suggested from the experience gained in the present work:

- In this investigation the sensitization was done only up to 15 hours, however sensitization studies can also be done for prolonged duration.
- All the tests in this investigation were carried out with positive mean stress value; however effect of negative mean stress on ratcheting behavior of the material can be studied.
- High temperature ratcheting studies can be done on this material.
- TEM studies of the tensile and ratcheted samples can be done to find any substructural variation.
- A comparative analysis of the effect of sensitization on mechanical properties and fatigue behavior of 304LN and non-conventional austenitic stainless steel can be done to comprehend the acceptability of the steel in critical sectors.

References

1) Singh, V. Physical mettalury, Third edition, Standard publications (2010).
2) Bhadeshia, H.K.D.H., Steels: Microstructure and properties, Third edition, Butterworth-Heinemann (2006).
3) Marshall P., Austenitic Stainless Steels; Microstructure and Mechanical Properties, Elsevier Applied Science Publishers (1984.).
4) Dutta R. S., De P. K., Gadiyar H. S., "The sensitization and stress corrosion cracking of nitrogen-containing stainless steels", Corrosion Science, Vol. 34 (1993), pp. 51–60.
5) Beneke R. and Sandenbergh R.F., "The influence of nitrogen and molybdenum on the sensitization properties of low-carbon austenitic stainless steels", Corrosion Science, Vol. 29 (1989), pp. 543–55.
6) Ghosh S., Kain V., Ray A., Roy H., Sivaprasad S., Tarafder S. and Ray K.K., "Deterioration in Fracture Toughness of 304LN Austenitic Stainless Steel Due to Sensitization", Metallurgical and Materials Transactions A, Vol. 40 (2009), Issue 12, pp. 2938-2949.
7) Ezzati M., Zeinoddini M., Fakheri J., "Uniaxial strain ratcheting behavior of dented steel tubular: An experimental study", Engineering Failure Analysis, Vol. 44 (2014), pp. 202–216.
8) Sarkar A., De P.S., Mahato J.K., Kundu A., Chakraborti P.C., "Effect of mean stress and solution annealing temperature on ratcheting behaviour of AISI 304 Stainless Steel", Procedia Engineering, Vol. 74 (2014), pp. 376 – 383.
9) Bain E. C., Aborn R. H., Rutherford J. J. B., "The nature of preventation of steels", Transaction of the American Society for Steel Treating, Vol. 21 (1933), pp. 481-509.
10) Cihal C., "Intergranular Corrosion of Steel and Alloys", Material Science Monographs, Elsevier, Amsterdam (1984), pp. 18-76.
11) Peckner D. and Bernstein I. M., "Handbook of Stainless Steels", McGraw-Hill, New York (1974), pp. 16-80.
12) Strauss B., Schor'rky H. and Hinnuber J., Z. Anorganische und Allgemeine Chemie 188, Vol. 309 (1930).

13) Stawstrom C. and Hillert M., "An improved depleted- zone theory of intergranular corrosion of 18-8 stainless steel", Journal of Iron Steel Institute, Vol. 207 (1969), pp.77-85.
14) Fullman R.L., "A thermodynamic model of the effects of composition on the susceptibility of austenitic stainless steels to intergranular stress corrosion cracking", Acta Metallurgica et Materialia, Vol. 30 (1982), pp. 1407-1415.
15) Devine T. M., "The mechanism of sensitization of austenitic stainless steel", Corrosion Science, Vol. 30 (1990), pp. 135-151
16) Gellinos, P.J. and Dejong, M. A., "Grain boundary oxidation and the chromium-depletion theory of intercrystalline corrosion of austenitic stainless steels", Corrosion Science, Vol. 7 (1967), pp.413-416.
17) Hall E. L., Briant C.L., "Chromium depletion in the vicinity of carbides in sensitized austenitic stainless steels", Metallurgical Transaction A, Vol. 154 (1984), pp. 793-811.
18) Watanabe T., "An approach to gain grain boundary design for strong and ductile polycrystals", Research Mechanica., Vol. 11 (1984), pp. 47–84.
19) Randle V., Owen G., "Mechanism of grain boundary engineering", Acta Metallurgica et Materialia, Vol. 54 (2006), pp. 1777-1783.
20) Kumar M., King W.E., Schwartz A.J., "Modifications to the microstructural topology in f.c.c. materials through thermo mechanical processing", Acta Metallurgica et Materialia, Vol.48 (2000), pp. 2081-2091.
21) Singh R., Chowdhury S.G., B. Ravi Kumar, Das S.K., De P.K. and Chattoraj I., "The importance of grain size relative to grain boundary character on the sensitization of metastable austenitic stainless steel", Scripta Materialia, Vol. 57 (2007), pp. 185–188.
22) Parvathavarthini N., Dayal R.K., Khatak H.S., Shankar V. and Shanmugam V., " Sensitization behavior of modified 316N and 316L stainless steel weld metals after complex annealing and stress relieving cycles", Journal of Nuclear Materials, Vol. 355 (2006), pp. 68–82.
23) Kain V., Chandra K., Adhe K.N., and De P.K., "Effect of cold work on low –temperature sensitization behavior of austenitic stainless steels", Journal of Nuclear Materials, Vol. 334 (2004), pp. 115–32.

24) Shankar P., Shaikh H., Sivakumar S., Venugopal S., Sundararaman D., and Khatak H.S., "Effect of thermal sging on the room temperature tensile properties of AISI type 316LN stainless steel", Journal of Nuclear Materials,Vol. 264 (1999), pp. 29–34.
25) Hilders O.A. and Santana M.G., "Metallography", Vol. 21 (1988), pp. 151–64.
26) Hertzberg R.W., "Deformation and Fracture Mechanics of Engineering Materials", Third edition, John Wiley & Sons, Singapore, (1989).
27) Bily M., "Cyclic Deformation and Fatigue of Metals", Materials Science Monographs 18, Elsevier, Amsterdam, London, New York, Tokyo, (1993).
28) Thompson N., Wadsworth N.J. and Louat N., "The origin of fatigue fracture in copper", Philosophical Magazine, Vol. 1 (1956), pp. 113-26.
29) Ellyin F., "Fatigue Damage, Crack Growth and Life Prediction", First edition, Chapman & Hall, UK, (1997).
30) Gao Q., Kang G.Z. and Yang X.J., "Uniaxial ratcheting of SS304 stainless steel at high temperatures: visco-plastic constitutive model", Theoretical and Applied Fracture Mechanics, Vol. 40 (2003), pp. 105–111.
31) Kang G., Gao Q. and Yang X., "Uniaxial cyclic ratcheting and plastic flow properties of SS304 stainless steel at room and elevated temperatures", Mechanics of Materials, Vol. 34 (2002), pp.145–159
32) Kujawski D., Kallianpur V., Kremple E., "An experimental study of axial creep, cyclic creep and relaxation of AISI type 304 stainless steel at room temperature", Journal of Mechanics Physics. Solids, Vol.28 (1980), pp.129–148.
33) Bari S. and Hassan T., "Anatomy of coupled constitutive models for ratcheting simulation", International Journal of Plasticity, Vol. 16 (2000), pp. 381–409.
34) Yoshida F., Itoh M., Shiratori E., "Effect of change of maximum stress and stress ratio on the cyclic-creep behavior", Bulletin of Japan Society of Mechanical Engineers, Vol. 24 (1981), pp. 507–514
35) Yoshida F., Yamamoto S., Itoh M., Ohmori M., "Biaxial strain accumulations in mechanical ratcheting", Bulletin of Japan Society of Mechanical Engineers, Vol. 27 (1984), pp. 2100–2106.
36) Rider R.J., Harvey S.J., Chandler H.D., "Fatigue and ratcheting interactions", International Journal of Fatigue, Vol. 17 (1995), pp. 507–511.

37) Kang G., Gao Q., Cai L., Yang X., Sun Y., "Experimental studies on uniaxial and multiaxial strain cyclic characteristics and ratcheting of 316L stainless steel", Journal of Material Science and Technology, Vol. 17 (2) (2001), pp. 219–223.

38) Varvani-Farahani A., "Fatigue–ratcheting damage assessment of steel samples under asymmetric multiaxial stress cycles", Theoretical and Applied Fracture Mechanics, Vol. 73 (2014), pp. 152–160.

39) Gupta S.K., Goyal S., Bhasin V., Vaze K.K., Ghosh A.K., Kushwaha H.S., "Prediction of ratcheting fatigue crack initiation in carbon steel", In Proceedings of the 4th Indo-German Theme Meeting on structural integrity of pressure retaining components; (2008).

40) Kang G.Z., Li Y.G., Zhang J., Sun Y.F., Gao Q., "Uniaxial ratcheting and failure behaviours of two steels", Journal of Theoretical and Applied Fracture Mechanics, Vol. 43 (2005), pp. 199-209.

41) Kulkarni S.C., Desai Y.M., Kant T., Reddy G. R., Parulekar Y. and Vaze K.K., "Uniaxial and biaxial ratchetting study of SA333 Gr.6 steel at room temperature", International Journal of Pressure Vessels and Piping, Vol. 80 (2003), pp. 179–185.

42) Xia Z., Kujawski D., Ellyin F., "Effect of mean stress and ratcheting strain on fatigue life of steel", International Journal of Fatigue, Vol. 18 (1996), pp.335-341.

43) Hassan T., Kyriakides S., "Ratcheting of cyclically hardening and softening materials: I. Uniaxial behaviour", International Journal of Plasticity, Vol.10 (1994), pp. 149-184.

44) Chen G., Chen X. and Niu C.D., "Uniaxial ratcheting behavior of 63Sn37Pb solder with loading histories and stress rates", Materials Science and Engineering A, Vol. 421 (2006), pp. 238–244.

45) Feaugas X. and Gaudin C., "Ratcheting process in the stainless steel AISI 316L at 300 K: an experimental investigation", International Journal of Plasticity, Vol. 20 (2004), pp. 643–662.

46) Nayar A., "The steel hand book", second edition, Tata MC Graw- Hill company limited, (2000).

47) Kozaczek K.J., Sinharoy A., Ruud C.O., and McIlree A.R., Modelling and Simulation in Materials Science and Engineering, 1995, Vol. 3, pp. 829–43.

48) Dieter G. E., Mechanical Metallurgy, SI metric edition, McGraw-Hill Book Company, Singapore, (1987).

49) Thomason P.F., “Ductile fracture by the growth and coalescence of microvoids of non-uniform size and spacing”, Acta Metallurgica et Materialia, Vol. 41 (1993), pp. 2127-2134.

50) Tvergaard, V., “Ductile fracture by cavity nucleation between larger voids”, Journal of Mechanics and Physics of Solids, Vol. 30 (1982), pp. 265–286.

51) Das, A., Sivaprasad, S.,Ghosh, M.,Chakraborti, P.C., Tarafder, S., “Morphologies and characteristics of deformation induced martensite during tensile deformation of 304 LN stainless steel”, Materials Science and Engineering A, Vol. 7 (2007) pp. 67-72.

52) Nagy, E., Mertinger, M., Tranta, F., Sólyom, J., “Deformation induced martensitic transformation in stainless steels”, Materials Science and Engineering A, Vol. 378 (2004), 308–313.

53) Dutta, K., Sivaprasad, S., Tarafder, S. and Ray, K. K., ”Influence of asymmetric cyclic loading on substructure formation and ratcheting fatigue behaviour of AISI 304LN stainless steel”, Materials Science and Engineering A, Vol. 527 (2010), pp. 7571–7579.

54) Kishor, R., Sahu, L., Dutta, K., Mondal, A. K., “Assessment of dislocation density in asymmetrically cyclic loaded non-conventional stainless steel using X-ray diffraction profile analysis”, Materials Science and Engineering A, Vol. 598 (2014), pp. 299-303.